Hyperglycemia and the Endothelium in Early Atherosclerosis

The Effects of Hyperglycemia on Early Endothelial Activation and Atherosclerotic Plaque Development

Robert Ballagh B.Sc. (Hons.)

A Thesis Submitted to the School of Graduate Studies in Partial Fulfillment of the Requirements for the Degree Master of Science

McMaster University MASTER OF SCIENCE (2018)

Hamilton, Ontario (Medical Science)

TITLE: Effects of Hyperglycemia on Early Endothelial Activation and Atherosclerotic Plaque Development

AUTHOR: Robert Alexander Douglas Ballagh, B.Sc. (McMaster University)

SUPERVISOR: Professor Geoff H. Werstuck

NUMBER OF PAGES: ix, 54

Lay Abstract

Cardiovascular disease is the leading cause of death in the world today. A major underlying cause of cardiovascular disease is atherosclerosis – a condition involving the thickening of the artery wall. Type I and II diabetes are each strong independent risk factors for atherosclerosis. The purpose of this study is to examine the effects of high blood glucose (hyperglycemia) on early events leading to atherosclerosis. This study found that hyperglycemia was not sufficient to promote atherosclerosis unless plasma cholesterol levels were also elevated. Hyperglycemia appeared to induce atherosclerosis by increasing the expression of factors responsible for recruiting white blood cells to the artery wall. This is consistent with the observation that hyperglycemic mice also had significantly more macrophages in the sites of plaque development. This study implicates one macrophage-recruitment factor in particular, vascular cell adhesion molecule (VCAM), as playing an important and unique role in the initiation of atherosclerosis by hyperglycemia. Therefore, VCAM is a possible target for the development of therapies to block or slow the development of atherosclerosis in individuals with diabetes.

Abstract

Cardiovascular disease is the leading cause of death in the world today. Atherosclerosis is the formation of plaque in the arteries and a major underlying cause of these fatalities. Type I and II diabetes are each strong independent risk factors for atherosclerosis. This study examines the effects of hyperglycemia on early atherosclerosis. Hyperglycemia did not promote atherosclerosis in the absence of hypercholesterolemia. Hyperglycemic mice demonstrated greater VCAM, but not ICAM, expression in regions of the endothelium susceptible to atherogenesis, prior to initiation of plaque development. Regions correlating to upregulation of VCAM exhibited a greater quantity of macrophages infiltrating the intima. This study suggests a unique and important role for VCAM in early atherosclerotic development and may explain the accelerated atherosclerotic plaque progression seen in hyperglycemic mice. This study also identifies VCAM as a potential target for the development of therapies to block or slow atherosclerotic plaque development in people with diabetes.

Table of Contents Page

Title Page i
Descriptive Note ii
Lay Abstract iii
Abstract iv
Table of Contents v
List of Figures and Tables vi
Acknowledgements vii
List of Abbreviations and Symbols viii
Declaration of Academic Achievement ix

Chapter 1: General Introduction 1
Cardiovascular Disease 1
Pathology of Atherosclerosis 1
Diabetes 2
Oxidative Stress 3
Endothelial Dysfunction 3
Non-Enzymatic Reactions 5
Mouse Models 6
VCAM 10
ICAM 10

Chapter 2: Hypothesis and Objectives 12
Hypothesis 12
Objectives 12

Chapter 3: Hyperglycemia and Atherosclerosis in ApoE$^{+/-}$ Mice 13
Abstract 13
Introduction 14
Methods 16
Results 21
Discussion 28
Conclusion 31

Chapter 4: Hyperglycemia and Endothelial Activation 32
Forward 32
Abstract 32
Introduction 34
Methods 36
Results 40
Discussion 58
Conclusion 62

Chapter 5: General Discussion **64**

Chapter 6: Future Work **67**

References **69**

List of Tables and Figures: **Page**

Chapter 3: Hyperglycemia and Atherosclerosis in ApoE$^{+/-}$ Mice

i. Fasting blood glucose of 25-week ApoE$^{+/-}$ Mice 22
ii. Cholesterol and Triglycerides in 25-week ApoE$^{+/-}$ Mice 23
iii. Plaque Volume of 25-week ApoE$^{+/-}$ Mice 25
iv. Blood Glucose and Plaque Volume in 25-week ApoE$^{+/-}$ Mice 26
v. Triglycerides, Cholesterol, and Plaque Volume in 25-week ApoE$^{+/-}$ Mice 27

Chapter 4: Hyperglycemia and Endothelial Activation

vi. Analysis of Glucose and Lipid Levels in Male ApoE$^{-/-}$ Mice 41
vii. Blood Glucose Levels in 10-week ApoE$^{-/-}$ mice 42
viii. Plaque Volume of ApoE$^{-/-}$ Mice 44
ix. Sample Images of VCAM Fluorescence 46
x. Endothelial VCAM Expression in ApoE$^{-/-}$ Mice 47
xi. Endothelial VCAM Expression in Ascending Aorta of ApoE$^{-/-}$ Mice 48
xii. VCAM Fluorescence Intensity in ApoE$^{-/-}$ Mice 49
xiii. Endothelial VCAM Expression in ApoE$^{+/-}$ Mice 50
xiv. Sample Images of ICAM-specific DAB Staining 52
xv. Endothelial ICAM Expression in ApoE$^{-/-}$ Mice 53
xvi. Endothelial VCAM Expression in Ascending Aorta of ApoE$^{-/-}$ Mice 54
xvii. Endothelial ICAM Expression in ApoE$^{+/-}$ Mice 55
xviii. Macrophage Recruitment in ApoE$^{-/-}$ Mice 57

Acknowledgements

My current success in my graduate studies would not be possible with the help and guidance from my supervisor, colleagues, friends and family. I would like to thank my supervisor, Dr. Geoff Hamilton Werstuck, for what has been an invaluable opportunity for academic achievement, personal growth, and scientific research. I would also like to acknowledge the work of my supervisor, Dr. Geoff H. Werstuck for his tireless support, input, and guidance in this study. Furthermore, I would like to acknowledge the efforts of our post-doctoral fellow Dr. Daniel Venegas-Pino, for providing insight, guidance, and additional unused specimens from his prior research. I would like to acknowledge the work of Dr. Peter Shi for his efforts in my training and his assistance drawing blood and harvesting mice for this study. I would like to acknowledge the efforts of my committee members, Dr. Bernardo Trigatti and Dr. Paul Kim, for their insight and direction and to thank the rest of the Werstuck, Kim, and Trigatti laboratories for their training, support and insight into this work.

	List of All Abbreviations and Symbols	Abbreviation
i.	Apolipoprotein E	ApoE
ii.	Apolipoprotein E homozygous knockout	$ApoE^{-/-}$
iii.	Apolipoprotein E heterozygous knockout	$ApoE^{+/-}$
iv.	Insulin 2	Ins2
v.	Insulin 2 Akita heterozygous knockout	$Ins2^{+/Akita}$
vi.	Vascular cell adhesion molecule 1	VCAM-1 or VCAM
vii.	Intercellular cell adhesion molecule 1	ICAM-1 or ICAM
viii.	Endothelial cells	EC
ix.	Low density lipoprotein	LDL
x.	Very low density lipoprotein	VLDL
xi.	High density lipoprotein	HDL
xii.	Low density lipoprotein receptor	LDLR
xiii.	Low density lipoprotein receptor homozygous knockout	$LDLR^{-/-}$
xiv.	Matrix metalloproteases	MMPs
xv.	Vascular smooth muscle cells	VSMCs
xvi.	Reactive oxygen species	ROS
xvii.	Endothelial nitric oxide synthase	eNOS
xviii.	Tetrahydrobiopterin	BH4
xix.	Dihydrobiopterin	BH2
xx.	Nitric oxide	NO
xxi.	Heparan sulphate	HS
xxii.	Glycated hemoglobin A_{1C}	HbA_{1C}
xxiii.	Histochemical	HC
xxiv.	Immunohistochemical	IHC
xxv.	Immunofluorescent	IF
xxvi.	Streptozotocin	STZ
xxvii.	Phosphate buffered saline	PBS
xxviii.	Advanced glycosylation end products	AGE
xxix.	Advanced glycosylation end products receptor	RAGE
xxx.	Tissue necrosis factor alpha	TNF-α
xxxi.	Platelet-derived growth factor	PDGF
xxxii.	Insulin-like growth factor 1	IGF-1
xxxiii.	Diaminobenzene	DAB
xxxiv.	Horseradish peroxidase	HRP
xxxv.	Very late antigen-4	VLA-4
xxxvi.	Cluster of differentiation 106	CD106
xxxvii.	Cluster of differentiation 54	CD54

Declaration of Academic Achievement

The experiments in this thesis were designed and conducted by Robert Alexander Douglas Ballagh, with the help of colleagues. Dr. Peter Shi assisted with harvesting and genotyping of the mice used in this study. Dr. Daniel Venegas-Pino provided insight and specimens remaining from prior, related studies and metabolic data pertaining to those mice. Dr. Geoff Hamilton Werstuck and Dr. Daniel Venegas-Pino provided valuable input that helped design the studies.

Chapter 1: General Introduction

Introduction

Atherosclerosis

Cardiovascular disease is the leading cause of death in the world today (Heron, 2018). Heart disease and stroke kill as many as 8.76 million and 6.24 million people respectively each year (Heron, 2018), including roughly 80% of all diabetic patients in North America (Ross, 1993). Atherosclerosis is the formation of plaque in the arteries and a major underlying cause of these fatalities (Heron, 2018). Atherosclerosis is initiated at sites of endothelial injury, which typically occurs at inner curvatures, bifurcations, and other regions of turbulent blood flow (Sud et al. 1984). Injured endothelial cells (ECs) express adhesive molecules that bind to circulating monocytes and recruit them to the site of inflammation[3]. Monocytes enter the intima and differentiate into macrophages, which engulf oxidized low-density lipoproteins (LDL), cholesterol, and modified LDL particles (Ross, 1993). These lipid-engorged macrophages become foam cells, accumulate in the intima, and form fatty streaks (Ross, 1993). Apoptotic foam cells collect to form necrotic regions of the plaque as atherosclerosis progresses (Sud et al. 1984). Matrix metalloproteases (MMPs) degrade collagen connective tissue, which disrupts cellular architecture and allows vascular smooth muscle cell (VSMC) migration into the intima (Vacek et al. 2015). VSMCs can further occlude the vessel, become foam cells, or undergo subsequent apoptosis (Vacek et al. 2015). If not rectified, these plaques can obstruct the arterial lumen and cause heart attacks, strokes, coronary heart disease, or angina (Sud et al. 1984).

When plaques rupture, blood comes into direct contact with the necrotic core initiating coagulation by activating the extrinsic pathway (Sud et al. 1984). This causes vessel occlusion, and potentially death (Sud et al. 1984). The specific molecular mechanisms by which hyperglycemia promote atherosclerosis are still being studied and this research is essential for the typically high-risk diabetic patients.

Diabetes

Diabetes is a complex heterogeneous group of metabolic conditions, often associated with dyslipidemia, hypertension and obesity (Noyman et al. 2002). Diabetes is the fifth leading cause of death globally and has been shown to dramatically increase atherosclerotic progression and cardiovascular risk (Das & Elbein 2006). Type I and II diabetes are both strong and independent risk factors for atherosclerosis (Aronson & Rayfield, 2002). More than 75% of hospitalizations for diabetic complications can be linked to cardiovascular problems (Aronson & Rayfield, 2002). Long-term hyperglycemia is now recognized as the primary causal factor in their pathogenesis (Aronson & Rayfield, 2002). Chronic elevated blood glucose causes several changes in the vascular endothelium that are believed to promote and accelerate atherosclerosis (Ross, 1993). Typical fasting blood glucose for humans is between 3.8 and 5.5mM (Das & Elbein 2006). Blood glucose higher than 7mM is classified as diabetic (Das & Elbein 2006). Hyperglycemia can facilitate the progression of heart disease through mechanisms that may involve oxidative stress, endothelial dysfunction, and non-enzymatic glycosylation of proteins and lipids (Aronson & Rayfield, 2002).

Oxidative Stress

Hyperglycemia may promote oxidative stress in several ways. Exposure of the arterial wall to glucose or free fatty acids increases superoxide production by the mitochondria (Nishikawa et al. 2000). This superoxide originates from the proton electrochemical gradient created by the electron transport chain of the mitochondria. This contributes significantly to the overall increase in reactive oxygen species (ROS) (Nishikawa et al. 2000). Glucose can also auto-oxidize when catalyzed by transition metals to produce free radical superoxide anions and peroxide (Karpen et al. 1985). Furthermore, hyperglycemia appears to compromise antioxidants such as vitamin C, glutathione, and vitamin E (Aronson & Rayfield, 2002); however, the mechanisms are yet unclear (Karpen et al. 1985). Studies of diabetic patients show marked drops in these antioxidants, including 40-50% reduction in vitamin C (Chen et al. 1983). This reduction in antioxidants and free radical production by glucose and mitochondria work in compliment to increase ROS. Despite these theories and some successful animal studies (Nishikawa et al. 2000) (Venegas-Pino et al. 2013) – antioxidant therapies have shown no beneficial effects toward cardiovascular disease in humans (Venegas-Pino et al. 2013) – so further research into this pathogenesis and treatment is essential.

Endothelial Dysfunction

The presence of ROS triggers two main pathways of endothelial dysfunction that precede atherosclerosis. The first is the uncoupling of endothelial nitric oxide synthase (eNOS) from its cofactor, tetrahydrobiopterin (BH4), via conversion to dihydrobiopterin (BH2) (Maron et al. 2013). Nitric oxide (NO) is a soluble gas continuously synthesized by eNOS and is a key regulator of vascular homeostasis (Maron et al. 2013). It regulates

platelet aggregation and adhesion, leukocyte-endothelial cell interactions, vascular tone, and local blood flow (Maron et al. 2013). eNOS can also produce superoxide, a potent ROS (Vásquez-Vivar et al. 1998). NO production is optimized when eNOS is coupled (dimerized via BH4) (Thum et al. 2007). Uncoupled eNOS only produces superoxide (Thum et al. 2007). This combination of compromised NO production and increased oxidative stress has a synergistic effect that adversely affects the vascular tone, increases arterial stiffness, and predisposes the vessel to vasospasm and cardiac ischemia (Matthys & Bult, 1997) (Baker et al. 2011). Perhaps most pertinently, loss of NO reduces inhibition of leukocyte adhesion (Baker et al. 2011).

A second pathway of endothelial dysfunction involves the activation of transcription factor NF-κB, the nuclear factor kappa-light-chain-enhancer of activated B cells (Funk et al. 2012). NF-κB is ubiquitous to nearly all animal cells and is a key regulator of the immune response to infection (Funk et al. 2012). It regulates the expression of pro-inflammatory genes, including intracellular adhesion molecule-1 (ICAM-1), vascular cell adhesion molecule-1 (VCAM-1), E-selectin, chemokines, and cytokines (Funk et al. 2012) in response to stimuli like ROS, cytokines, heavy metals, oxidized LDL, and bacterial or viral antigens (Funk et al. 2012). ICAM-1, VCAM-1, and E-selectin recruit monocytes to the site of inflammation (Funk et al. 2012). Intimal monocytes differentiate into macrophages, which become engorged with lipids in the subendothelial space (Sud et al. 1984). Lipid engorged macrophage foam cells undergo apoptosis and contribute to the growth of the necrotic core (Sud et al. 1984). Hyperglycemia's role in increasing oxidative stress is one way it increases the activation of NF-κB and pathological progression of atherosclerosis (Funk et al. 2012).

Hyperglycemia also damages other endothelial factors. Proteoglycans are a major component of the extracellular matrix and are found on the endothelial cell membrane (Gabbay et al. 1977). They are chemically diverse macromolecules composed of a protein core and branching glycosaminoglycans (GAGs) (Gabbay et al. 1977). Proteoglycans and collagen form large complexes to create cartilage, and heparan sulphate (HS) proteoglycans regulate blood coagulation, angiogenesis, developmental processes, and tumour metastasis (Gabbay et al. 1977). Hyperglycemia and related oxidative stress have been shown to upregulate heparanase, reduce HS, and damage other GAGs (Gabbay et al. 1977).

Non-Enzymatic Reactions

Some effects of hyperglycemia are irreversible and lead to progressive cell dysfunction[6]. Symptoms and complications of hyperglycemia can persist despite a return to normoglycemic conditions (Aronson & Rayfield, 2002). Non-enzymatic reactions between glucose and proteins or lipids can facilitate this metabolic memory (Aronson & Rayfield, 2002). Glucose forms glycosylation products with vulnerable amino groups of circulating or vessel wall proteins (Aronson & Rayfield, 2002). These products are initially reversible, but eventually rearrange to form stable biomolecules called Schiff bases and eventually Amadori products (Aronson & Rayfield, 2002). One well-known product, glycated haemoglobin A_{1C} (HbA_{1C}), is used in annual testing for diabetics as a metric for long-term blood glucose (Brownlee et al. 1988). Haemoglobin has a life span of 80-120 days in a healthy adult (Brownlee et al. 1988) and thus, medical professionals can measure the amount of HbA_{1C} in the blood to determine a person's average blood glucose level for the previous 2-3 months (Brownlee et al. 1988). Unfortunately, not all tissues have similar cell half-lives. Some long-lived proteins, like vessel wall collagen, can rearrange over time

to create advanced glycosylation end products (AGEs) (Feener & King, 1997). These AGEs are stable and near irreversible (Feener & King, 1997). They accumulate with increasing blood glucose and time of exposure (Feener & King, 1997) increasing oxidative stress (Brownlee et al. 1988).

AGEs accelerate atherosclerosis through non-receptor mediated mechanisms in the extracellular matrix and receptor-mediated mechanisms (AGE-RAGE) (Brownlee et al. 1988). The AGE-RAGE interaction can promote inflammation by inducing the secretion of cytokines, such as tumour necrosis factor-α (TNF-α), as well as induce cellular proliferation stimulating monocyte secretion of platelet-derived growth factor (PDGF) and insulin-like growth factor 1 (IGF-1) (Brownlee et al. 1988). Additionally, AGEs stimulate endothelial dysfunction, demonstrated by increasing permeability of endothelial cell monolayers, procoagulant activity through tissue factor expression, increased expression of adhesion molecules like VCAM and ICAM, and intracellular oxidative stress (Brownlee et al. 1988; Feener & King, 1997; Funk et al. 2012). These mechanisms increase endothelial dysfunction, recruitment of macrophages to sites of atherosclerotic development, and contribute to the oxidative stress characteristic of hyperglycemia (Funk et al. 2012).

Mouse Models

Mice serve as useful models for studying cardiovascular disease. Mice do not normally develop atherosclerosis, even when fed a high-fat diet (Beckman et al. 2002; Zadelaar et al. 2007). Existing mouse models contain a recessive loss-of-function mutation in the gene for the low-density lipoprotein receptor (LDLR) or apolipoprotein E (ApoE) (Wu & Huan, 2007). These mutations interfere with normal lipid clearance and render the mice susceptible to atherogenesis (Wu & Huan, 2007; Zadelaar et al. 2007).

$ApoE^{-/-}$ mice are a homozygous knockout of ApoE and develop plaques spontaneously, even when fed a normal diet (Nguyen et al. 2009; Wu & Huan, 2007). ApoE is an apolipoprotein component of high-density lipoproteins (HDL), very low-density lipoproteins (VLDL), and chylomicron remnants that participates in their metabolism and clearance (Barber et al. 2005). ApoE mediates their clearance from the plasma compartment through interaction with cell surface receptors, especially those of LDL (Barber et al. 2005). ApoE also promotes cellular endocytosis of lipoproteins by binding heparin sulphate proteoglycans (Barber et al. 2005). This reduces plasma cholesterol levels and subsequent risk of plaque formation (Barber et al. 2005). Compromising the activity of ApoE increases circulating proatherogenic VLDL and renders mice much more susceptible to atherosclerosis (Barber et al. 2005; Beriault et al. 2016).

In order to study the effects of diabetes in mice, hyperglycemia must be induced in the mouse model. Normal fasting blood glucose in humans is between 3.8 and 5.5 mM (Wu & Huan, 2017). Fasting blood glucose levels are slightly higher in mice than in humans. Our lab defines murine normoglycemia as a level below 9mM. Mice with blood glucose levels >13mM are classified as diabetic hyperglycemia (Barber et al. 2005). Hyperglycemia is typically induced in one of two ways: i) intraperitoneal injection with streptozotocin (STZ), a toxin selective for pancreatic beta cells, or more recently, ii) the mutation of one copy of the gene insulin 2 (*Ins2*), a homologue of human insulin (Venegas-Pino et al. 2016).

$Ins2^{+/Akita}$ is a commonly available mouse line with a dominant mutation that spontaneously induces early-onset diabetes without compromising fertility (Zhang et al. 1994). This makes it an excellent candidate for a genetic model of diabetes. The mutation

causes pancreatic β-cell apoptosis and insulin deficiency (Venegas-Pino et al. 2016). By inducing diabetes genetically, this model eliminates potential confounding effects associated with the administration and other physiological effects of streptozotocin, such as hepatotoxicity and nephrotoxicity (Graham et al. 2011).

While our lab has shown $Ins2^{+/Akita}$ to be preferable to streptozotocin, there are some things that should be noted about the model. Jackson Laboratories show that $Ins2^{+/Akita}$ mice demonstrate significantly elevated levels of glutathione S-transferase mRNA, increased sphingosine-1-phosphate and plasma concentrations of valine, leucine, isoleucine, alanine, citrulline, proline, and total branched chain amino acids (Jackson Laboratory, 2018). Akita mice also have general reductions in nervonic acid, containing ceramide, sphingomyelin, and reductions in cerebrosides, and sphingolipids in the liver and heart. Aged $In2^{+/Akita}$ mice show gait disturbance, hyperphagia, anxiety, and decreased sensory nerve conduction velocity but no reduction in learning or memory (Jackson Laboratory, 2018). They have a shorter lifespan, typical of hyperglycemic models, with an average life span of 305 days, less than half the longevity of normoglycemic male mice of the same background, 690 days (Jackson Laboratory, 2018). The heterozygous model of $Ins2^{+/Akita}$ used for this study is most common, as untreated homozygotes rarely survive beyond 12 weeks (Jackson Laboratory, 2018). This study intends to look at both early and late stages of atherosclerosis, beyond 12 weeks. Other methods of inducing hyperglycemia are available, including various genetic, chemical, and spontaneous autoimmune methods, however the $Ins2^{+/Akita}$ model has proven to be one that is reliable and effective over the course of several studies conducted by our lab (Barber et al. 2005; Martin-Body et al, 1985).

Our lab has previously created the ApoE$^{-/-}$ Ins2$^{+/Akita}$ mouse (Martin-Body et al, 1985; Venegas-Pino et al. 2016). Males developed chronic hyperglycemia while females showed transient hyperglycemia between 5 and 10 weeks of age, after which blood glucose levels normalized (Venegas-Pino et al. 2016). The underlying reason for this sex-specific effect is currently under investigation in the Werstuck lab (Venegas-Pino et al. 2016). The chronic hyperglycemia seen in males significantly exacerbated atherosclerosis and the transient hyperglycemia in females also caused an increase in plaque development (Venegas-Pino et al. 2016).

The experiments proposed in this study will utilize the ApoE homozygous knockout strain (ApoE$^{-/-}$) for both control and experimental groups. These experiments will also use the heterozygous ApoE mutant (ApoE$^{+/-}$). The Werstuck lab has previously found that heterozygous ApoE$^{+/-}$ mice do not have significantly elevated plasma lipid levels, compared to C57Bl6 mice, and do not develop large plaques (Martin-Body et al, 1985). These experiments are based upon the results of our lab's previous observations of potential plaque development in hyperglycemic ApoE$^{+/-}$ Ins2$^{+/Akita}$ mice (Martin-Body et al, 1985). This study intends to determine if hyperglycemia significantly increases early atherosclerosis or incites initiation of plaque formation in the normolipidemic ApoE$^{+/-}$ mouse model. The hyperglycemia will be induced genetically, via the Ins2$^{+/Akita}$ mutation (Martin-Body et al, 1985).

This study will also examine endothelial activation in hyperglycemic mice compared to normoglycemic controls, using both the ApoE$^{+/-}$ and ApoE$^{-/-}$ mouse models, and will focus on early plaque development. Aortic cross sections will be analyzed through

histochemical (HC), immunohistochemical (IHC), and immunofluorescent (IF) staining, to compare expression of conventional markers of endothelial activation, VCAM and ICAM.

VCAM

Vascular cell adhesion molecule 1 (VCAM-1) or cluster of differentiation 106 (CD106) is a cell surface sialoglycoprotein of mice and humans encoded by the *VCAM1* gene (Cybulsky et al. 2001; Khalfaoui et al. 2008; Watanabe et al. 1989). It is part of the immunoglobin (IG) superfamily (Ceriello et al. 1998; Khalfaoui et al. 2008). VCAM-1 mediates the adhesion of leukocytes to the vascular endothelium by binding to two leukocyte integrins, α4β1 and α4β7 (Newham et al. 1997; Yang et al. 2013). It has also been shown to interact with membrane-organizing extension spike protein and Ezrin, however it functions primarily by binding to integrin α4β1, also known as very late antigen-4 (VLA-4) (Newham et al. 1997). The promoter region for the *VCAM1* gene contains binding sites for NF-κB. NF-κB upregulates gene transcription of *VCAM1* in response to TNFα and IL-1 (Barreiro et al. 2002; Cybulsky et al. 2001).

ICAM

Intercellular adhesion molecule 1 (or ICAM-1) or cluster of differentiation 54 CD54 is a cell surface glycoprotein expressed primarily on endothelial cells and leukocytes, much like VCAM-1 (Cybulsky et al. 2001; Marlin & Springer, 1987). It is encoded by the *ICAM1* gene and binds to integrins CD11a/CD18 or CD11b/DC18 present on the cell surface of leukocytes (Cybulsky et al. 2001). The binding of ICAM and these integrins provides the firm adhesion necessary for leukocytes to extravasate through the endothelium to sites of inflammation and endothelial dysfunction (Cybulsky et al. 2001; Khalfaoui et al. 2008). Recent evidence by Cybulsky et al. suggests a key role for VCAM

in the initiation of atherosclerosis in hyperglycemic mice that is not seen with ICAM (Cybulsky et al. 2001). This study examines each endothelial recruitment factor to provide a better understanding of the mechanisms behind the hyperglycemia-induced onset of atherosclerosis.

Chapter 2: Hypothesis and Objectives

Hypothesis

We hypothesize that hyperglycemia initiates and accelerates the development of atherosclerosis in both normolipidemic and dyslipidemic mice by a mechanism that involves induction of VCAM and/or ICAM expression.

Objectives

This study will examine aortic cross sections from mouse models of hyperglycemia ($Ins2^{+/Akita}$) and normoglycemic cohorts ($Ins2^{+/+}$). The first phase of the project will determine if normolipidemic $ApoE^{+/-}Ins2^{+/Akita}$ mice develop significantly larger atherosclerotic lesions than $ApoE^{+/-}$ mice. Plasma will be collected to determine plasma triglyceride and cholesterol concentrations (Venegas-Pino et al. 2016). Plaque volume will be visualized with trichrome staining, quantified, and compared (Venegas-Pino et al. 2013). The second phase compares markers of endothelial activation between hyperglycemic and normoglycemic mice for both $ApoE^{+/-}$ and $ApoE^{-/-}$ mouse models. This study will further characterize this new heterozygous strain of hyperglycemic mice and increase our understanding of the role of hyperglycemia in endothelial activation in both $ApoE^{+/-}$ and $ApoE^{-/-}$ mouse models.

Chapter 3: Hyperglycemia and Atherosclerosis in ApoE$^{+/-}$ Mice

Abstract

Objective

This study investigates the effects of hyperglycemia on plaque volume in the normolipidemic ApoE$^{-/-}$ mouse model. We showed that the hyperglycemic ApoE$^{+/-}$ Ins2$^{+/Akita}$ mice demonstrated no significant differences in lipids or plaque volume from their normoglycemic ApoE$^{+/-}$ counterparts, at 25 weeks. Recent evidence in this lab suggested that hyperglycemic ApoE$^{+/-}$ mice may develop plaques and normoglycemic ApoE$^{+/-}$ mice do not. This mouse model does not demonstrate dyslipidemia and has shown persistent hyperglycemia in female mice, which is not present in the ApoE$^{-/-}$ model. In this study, we used the Ins2$^{+/Akita}$ mouse model to look at the effects of hyperglycemia in the absence of dyslipidemia on both male and female ApoE$^{+/-}$ mice.

Approach and Results

Blood glucose was measured with a glucometer for each mouse and total plasma cholesterol and triglycerides levels were determined using treated with infinity reagent chromogens and quantification with absorption chromatography (Maeda, 2011; Shimomura et al. 1999). Hearts of ApoE$^{+/-}$ mice were cut parallel to and 5mm below the aortic sinus and encased in paraffin blocks (Venegas-Pino et al. 2013). These blocks were sectioned and the sections stained with Mason's trichrome to visualize endothelium, collagen, and plaque (Venegas-Pino et al. 2013). Stained sections were imaged at 10x magnification, quantified with ImageJ tracing software, and final plaque volumes were calculated (Venegas-Pino et al. 2013). These volumes were compared statistically with Man-Whitney *U* tests and Kruskal Wallace *H* tests if they failed the D'Agostino-Pearson

omnibus normality test, or Student's *T* tests and One-way ANOVA if they were normally distributed (Poirier et al. 2005).

Conclusions

ApoE$^{+/-}$ Ins2$^{+/Akita}$ mice had significantly elevated blood glucose and no differences in plasma lipids. There were no significant differences in plaque volume between ApoE$^{+/-}$ and ApoE$^{+/-}$ Ins2$^{+/Akita}$ mice. These results suggest that hyperglycemia independent of dyslipidemia is not sufficient to induce accelerated atherosclerosis.

Introduction

Unlike humans, mice have a very atheroprotective lipid profile (Maeda, 2011; Shimomura et al. 1999). Mice typically display low plasma cholesterol and a lipid profile that is rich in the anti-atherogenic HDL and low in the pro-atherogenic VLDL and LDL (Maeda, 2011; Venegas-Pino et al. 2013). Mice also live very short lives, averaging between 2 and 3 years, which is not enough time for plaques to form like we see in humans (Poirier et al. 2005). Humans develop plaques over the span of dozens of years, so a model reflecting this progression in mice would need to accelerate their plaque development (Sud et al. 1984). First developed by Nobuyo Maeda, ApoE$^{-/-}$ mice are a well-established mouse model of atherosclerosis; characterized by chronic hypercholesterolemia (Maeda, 2011). ApoE is an important ligand for receptors that clear LDL and chylomicrons from the plasma (Poirier et al. 2005; Shimomura et al. 1999). Cholesterol-rich remnants accumulate in the circulation when ApoE is knocked out, which promotes deposition of lipids in the subendothelial space and the resultant pathogenesis of atherosclerosis (Maeda, 2011; Shimomura et al. 1999).

A study by Zhang et al. 2008 showed a 5-fold increase in murine plasma cholesterol and plaques in the proximal aorta by 3 months (Zhang et al. 1992). These plaques continued to grow and caused severe occlusion by 8 months (Zhang et al. 1992). Moreover, these results were obtained with a normal chow diet (Zhang et al. 1992). $ApoE^{-/-}$ mice develop spontaneous plaques without the need for a high fat diet, which is required by models like $LDLR^{-/-}$ (Maeda, 2011; Poirier et al. 2005; Zhang et al. 1992). This allows us to observe the effects of chronic hypercholesterolemia in mice without excess dietary fat (Poirier et al. 2005; Zhang et al. 1992).

While this is convenient, it should be noted that there is a complication with the $ApoE^{-/-}$ mouse model when considering female mice in studies of hyperglycemia (Shea et al. 2004; Venegas-Pino et al. 2016). Female $ApoE^{-/-}$ mice demonstrate transient hyperglycemia that presents early around 5 weeks of age, but then returns to normal healthy murine levels by 10 weeks (Venegas-Pino et al. 2016). This presents a challenge for experiments testing the effects of hyperglycemia on female mice (Shea et al. 2004; Venegas-Pino et al. 2016), however this transient hyperglycemia appears to be unique to the homozygote ($ApoE^{-/-}$) (Venegas-Pino et al. 2016). The return to normal blood glucose levels is not observed in $ApoE^{+/-}$ mice (Venegas-Pino et al. 2016).

Instead, female $ApoE^{+/-}$ mice retain a significantly elevated hyperglycemia at both 10 and 15 weeks of age (Venegas-Pino et al. 2016). Additionally, $ApoE^{+/-}$ mice show relatively normal plasma lipid levels (Poirier et al. 2005; Shea et al. 2004; Venegas-Pino et al. 2016). During the course of the study explaining this phenomenon, by Venegas-Pino et al. in our lab, experimenters saw some evidence of larger plaques in the hyperglycemic $ApoE^{+/-}$ mice than those in their normoglycemic $ApoE^{+/-}$ counterparts (Poirier et al. 2005;

Venegas-Pino et al. 2016). While these plaques were very small, even at 25 weeks, this could suffice as a useful way to assess the effects of hyperglycemia in the absence of dyslipidemia and in female mice (Venegas-Pino et al. 2016). This study was designed to test the viability of this model in assessing the accelerating effects of hyperglycemia on the development of atherosclerosis and to observe the effects of hyperglycemia on atherosclerotic inception and acceleration in a model without dyslipidemia.

Methods

Harvesting and Sectioning

All ApoE$^{+/-}$ mice were fed a normal chow diet and harvested at 25 weeks of age (Maeda, 2011; Poirier et al. 2005; Venegas-Pino et al. 2016). ApoE$^{-/-}$ mice were fed a normal chow diet and harvested at 5, 10, 15, and 25 weeks of age (Venegas-Pino et al. 2016). To quantify the extent of atherosclerotic development: hearts were perfused with phosphate buffered saline (PBS), harvested, fixed in 10% formalin, processed in a tissue processor, and encased in paraffin blocks (Venegas-Pino et al. 2013). The paraffin-encased tissue was trimmed at 10 micrometers until initial signs of the first leaflet of the aortic valve were observed (Venegas-Pino et al. 2013). The block was then reoriented until the second leaflet became apparent (Venegas-Pino et al. 2013). When at least two of the three aortic valve pouches were visible, the microtome was then switched to section at 4.5 micrometers and sections were fixed to slides via a hot water bath, set to 45 degrees Celsius (Venegas-Pino et al. 2013). Sections were distributed over 10 slides in staggered order (slide 1, slide 2… slide 10, slide 1…) running left to right and top to bottom (Venegas-Pino et al. 2013; Venegas-Pino et al. 2016). Sections were taken until the aortic valve pouches were no

longer observed (Venegas-Pino et al. 2013; Venegas-Pino et al. 2016). Due to the small size of plaques in $ApoE^{+/-}$ specimens, this technique was adapted with the second batch of mice so that sectioning would begin at the appearance of the first aortic valve pouch and no reorientation would occur (Venegas-Pino et al. 2013). This was an attempt at reducing the likelihood of missing plaques (Venegas-Pino et al. 2013; Venegas-Pino et al. 2016). Conversely, $ApoE^{-/-}$ hearts were all sectioned until at least 2 aortic valve pouches were visible, as described above (Venegas-Pino et al. 2013; Venegas-Pino et al. 2016).

Plaque and Lipid Quantification

All mice were sectioned at a thickness of 4.5um (Venegas-Pino et al. 2013; Venegas-Pino et al. 2016). Aortic sinuses were fully sectioned after 8-12 sections (Venegas-Pino et al. 2013). $ApoE^{+/-}$ sections were stained with Mason's trichrome (Venegas-Pino et al. 2013). Mason's trichrome stains connective tissue blue, nuclei dark red/purple, and cytoplasm pink (Gerlis et al. 1985; Venegas-Pino et al. 2013). The first slide of each specimen's set was stained unless significant damage necessitated other slides be used. Once stained, slides were imaged and plaque area quantified using ImageJ software (Gerlis et al. 1985; Venegas-Pino et al. 2013). Plaque volumes were calculated from sequential measurements of area on adjacent sections (see statistical analysis). Plaque areas of each section were defined as the sum of all plaque in all aortic valve pouches (Venegas-Pino et al. 2013; Venegas-Pino et al. 2016). The average area of two adjacent sections was multiplied by the thickness of the sections to determine volume of plaque within the first of the two sections (Venegas-Pino et al. 2013; Venegas-Pino et al. 2016). Volumes were tested for normality with the D'Agostino-Pearson omnibus normality test (D'Agostino et al. 1990) compared via the nonparametric Mann-Whitney *U* test if they

were not normally distributed (McKnight & Najab, 2010), or a Student's *t*-test if they were normally distributed (Haynes, 2013), between $ApoE^{+/-}$ $Ins2^{+/Akita}$ and $ApoE^{+/-}$ groups. No data set was normally distributed, so all were compared with Mann-Whitney *U* tests (D'Agostino et al. 1990; McKnight & Najab, 2010).

To better understand the context of disease pathogenesis, lipid profiles, cholesterol, and triglyceride levels were quantified with Infinity reagents (Rashid et al. 2005; Venegas-Pino et al. 2016). Quantitative determinations of cholesterol and triglyceride levels in vitro were each conducted in 96-well plates and compared against a standard curve established via serial dilution (Rashid et al. 2005; Venegas-Pino et al. 2016). Cholesterol and triglyceride reagents respectively were added to the plasma to facilitate concentration-dependent absorbance at 500nm (Rashid et al. 2005; Venegas-Pino et al. 2016). Colorimetric assays were conducted on the plates, specified to a 500nm wavelength, in a spectrophotometer (Rashid et al. 2005; Venegas-Pino et al. 2016). Absorbance was converted to concentration by extrapolating from the standard curve (Rashid et al. 2005; Venegas-Pino et al. 2016). Concentrations were compared between 25-week old male and female, $ApoE^{+/-}$ and $ApoE^{+/-}$ $Ins2^{+/Akita}$ groups, as well as male $ApoE^{-/-}$, and $ApoE^{-/-}$ $Ins2^{+/Akita}$ at 5, 10, 15, and 25 weeks of age (Black et al. 2000; Venegas-Pino et al. 2013; Venegas-Pino et al. 2016).

Lipid profiles were estimated by pooling plasma from all specimens within each group, for the $ApoE^{+/-}$ mouse model (Coleman et al. 1984; Thum et al. 2007). These mixtures were subjected to size-exclusion chromatography to separate HDLs, LDLs and VLDLs into a gradient plotted on a 96-well plate (Thum et al. 2007). Colorimetric assays were performed in a spectrophotometer following the addition of the cholesterol reagent

(Rashid et al. 2005). Absorbance was set to 500nm in the spectrophotometer and intensities obtained were converted to concentrations via the standard curve (Rashid et al. 2005). These mixtures were compared between all $ApoE^{+/-}$ groups.

Plaque volume for $ApoE^{-/-}$ mice was much larger than $ApoE^{+/-}$ mice and easier to visualize with staining methods like DAB IHC staining (Maeda, 2011; Ruifrok & Johnston, 2001; Venegas-Pino et al. 2013). It was quantified from aortic sinus cross-sections previously stained with DAB to measure ICAM (Ruifrok & Johnston, 2001). The larger plaque size made it possible and practical to quantify with this method (Maeda, 2011; Ruifrok & Johnston, 2001; Venegas-Pino et al. 2013).

Statistical analysis

Plaque volume was calculated from serial 2D images of aortic sinus sections by multiplying the average area of adjacent sections by the section thickness (Venegas-Pino et al. 2013). This was then converted from um^3 to mm^3. This process used the following equation:

$$V = T\frac{(S_n + S_{n+1})}{2}$$

Where V is volume, T is section thickness, S_n is the first section of two adjacent sections and S_{n+1} is the next adjacent section further along the aortic sinus or ascending aorta (Venegas-Pino et al. 2013). All sections were taken at a thickness of 4.5 um (Venegas-Pino et al. 2013; Venegas-Pino et al. 2016). All measurements were then converted from um^3 to mm^3.

$$V = 4.5\frac{(S_n + S_{n+1})}{2}10^{-9}$$

This calculation was applied to every adjacent pair of sections from the 1st to 10th section in order to calculate the volume of plaque between each pair (i.e. 1&2, 2&3, 3&4 … 9&10) (Venegas-Pino et al. 2013). Plaques did not present past the 10^{th} section in $ApoE^{+/-}$ mice and so plaque volume was only measured up to 10 sections deep (450um) (Venegas-Pino et al. 2013). All of these sequential volumes calculated were summed to find the total plaque volume for each mouse (Venegas-Pino et al. 2016). These were then compared between groups.

Groups were tested for normal distribution with D'Agostino & Pearson omnibus normality tests (D'Agostino et al. 1990). Small sample sizes ($n<8$) often give false positives for normality tests (D'Agostino et al. 1990; Haynes, 2013; McKnight & Najab, 2010). It is more reliable to use non-parametric analyses in these cases (D'Agostino et al. 1990; McKnight & Najab, 2010). For this reason, samples that did not present with normal distribution, or had sample sizes below 8, were analyzed with non-parametric analyses (D'Agostino et al. 1990; McKnight & Najab, 2010). Comparisons between two groups were analyzed with non-parametric Mann-Whitney *U* tests (McKnight & Najab, 2010). Comparisons between multiple groups were conducted with non-parametric Kruskal-Wallis *H* tests (Heiberger & Neuwirth, 2009; McKnight & Najab, 2010). Normally distributed data was analyzed with t-tests for comparisons between two groups (Ruifrok & Johnston, 2001) and one-way ANOVA for multiple comparisons (D'Agostino et al. 1990; Heiberger & Neuwirth, 2009).

For all statistical analyses, outliers were defined as any point of data outside of the respective interquartile range for that data (Rousseeuw & Leroy, 2005). Outliers were identified using this method digitally with Excel software and were exclude from analysis

(Rousseeuw & Leroy, 2005). Interquartile range and outliers were recalculated each time data was added or removed (Rousseeuw & Leroy, 2005).

Results

Metabolic Parameters

25-week male ApoE+/- mice carrying the Ins2+/Akita mutation had significantly elevated fasting blood glucose levels relative to age and sex-matched ApoE+/- controls (Figure 1) ($P<0.0001$) (n=7,11). Blood glucose in female ApoE+/- Ins2+/Akita mice was also significantly elevated relative to ApoE+/- mice ($P=0.0168$) (n=7-10).

$ApoE^{+/-}$ $Ins2^{+/Akita}$ mice had no significant difference in fasting plasma cholesterol levels relative to their $ApoE^{+/-}$ counterparts (Figure 2) (n=6). Female $ApoE^{+/-}$ $Ins2^{+/Akita}$ mice showed significantly elevated plasma triglycerides relative to $ApoE^{+/-}$ females ($p=0.0071$) (n=6) however no significant difference was observed in male mice (Figure 2) (n=6).

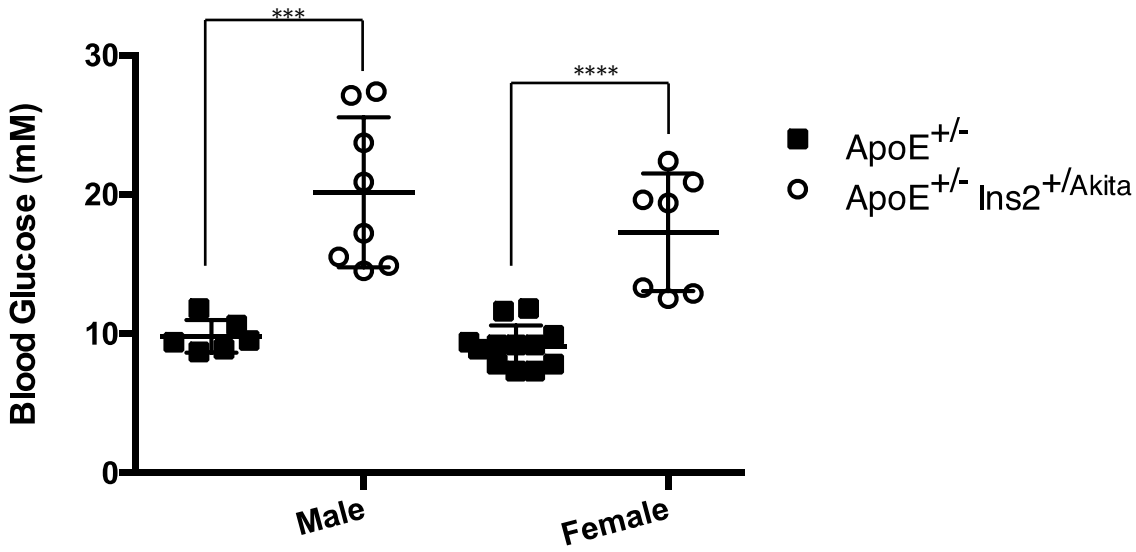

Figure 1: *Fasting blood glucose of 25-week ApoE$^{+/-}$ Mice:* Blood glucose was significantly elevated for both male and female ApoE$^{+/-}$ Ins2$^{+/Akita}$ mice relative to age-matched ApoE$^{+/-}$ controls (p=0.007 and <0.0001 respectively) (n=6,7,12,7).

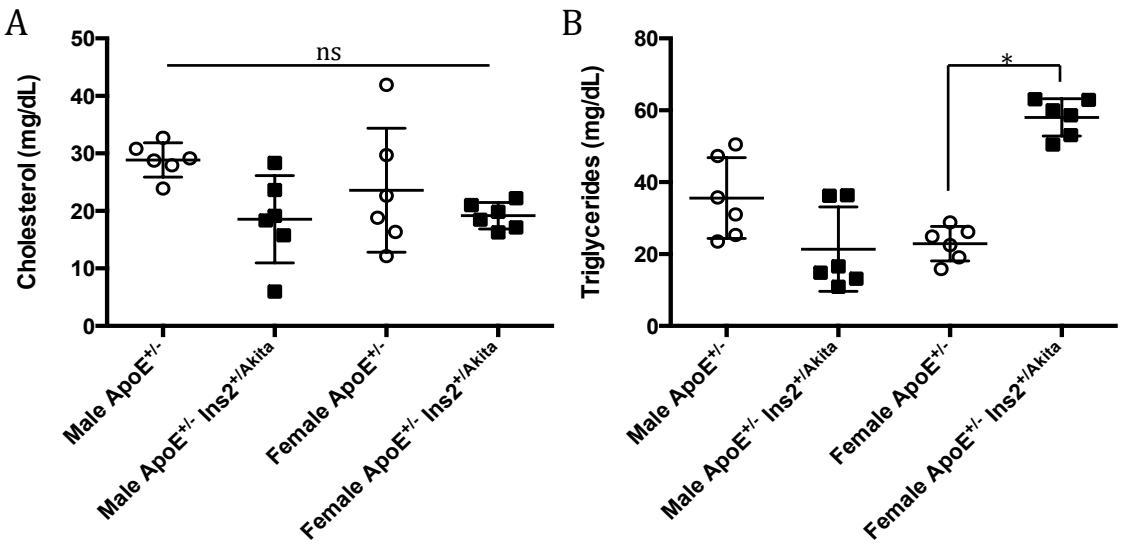

Figure 2: Cholesterol and Triglycerides in 25-week ApoE+/- mice. A. Plasma cholesterol and B. triglyceride concentrations for ApoE+/- and ApoE+/- Ins2+/Akita, male and female mice at 25 weeks of age. Groups were compared with one-way ANOVA. There were no significant differences in plasma cholesterol between ApoE+/- and ApoE+/- Ins2+/Akita mice in males or females (n=6). There were no significant differences in plasma triglycerides for male ApoE+/- and ApoE+/- Ins2+/Akita mice (n=6), however female ApoE+/- In2+/Akita mice had significantly higher plasma triglycerides than their ApoE+/- counterparts (p=0.0071) (n=6).

Atherosclerotic Plaque

The heart and ascending aorta from each group of mice was sectioned and the aortic sinus was stained with Mason's trichrome to visualize the cellular architecture by contrasting plaques (pink and red) against the blue collagen of the aortic wall (Figure 3a-d) (Sud et al. 1984). Very small lesions (fatty streaks) were observed in at least some mice from each of the ApoE+/- groups, however there were no significant differences in plaque volume between any of the male or female ApoE+/- of ApoE+/- Ins2+/Akita mice (n=8-12) (Figure 3e). One male ApoE+/- and one female ApoE+/- Ins2+/Akita mouse had plaques four times larger than any other specimen and fifteen times larger than average. These mice were excluded as outliers, following calculation specified above.

There was no significant correlation between plaque volume and fasting blood glucose concentration in A) male ApoE+/- or B) female ApoE+/- groups (Figure 4) (n=8-12, 9-10). There was also no significant correlation between plaque volume and fasting plasma cholesterol or triglycerides (Figure 5) (n=17,19).

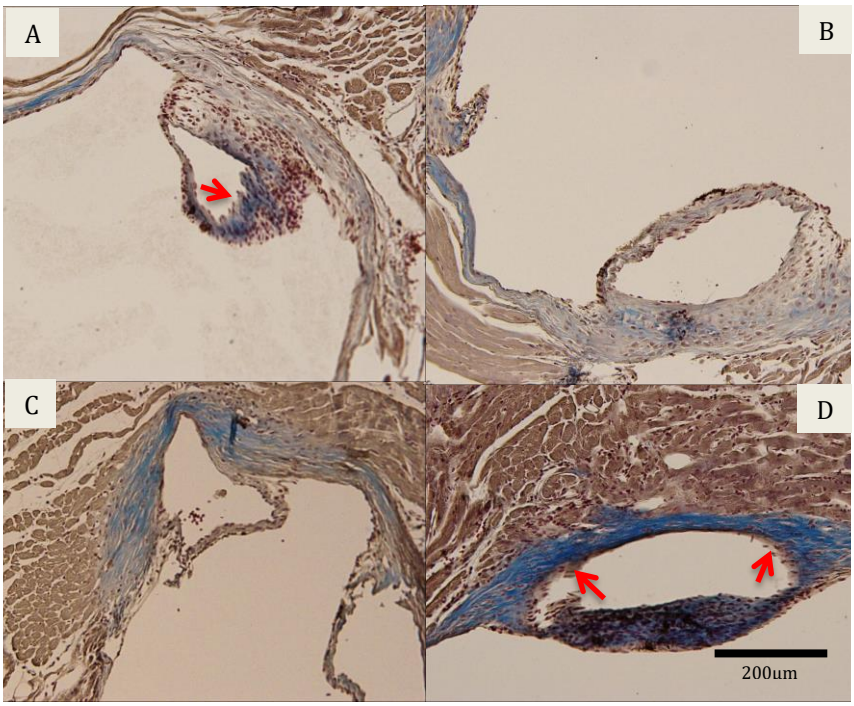

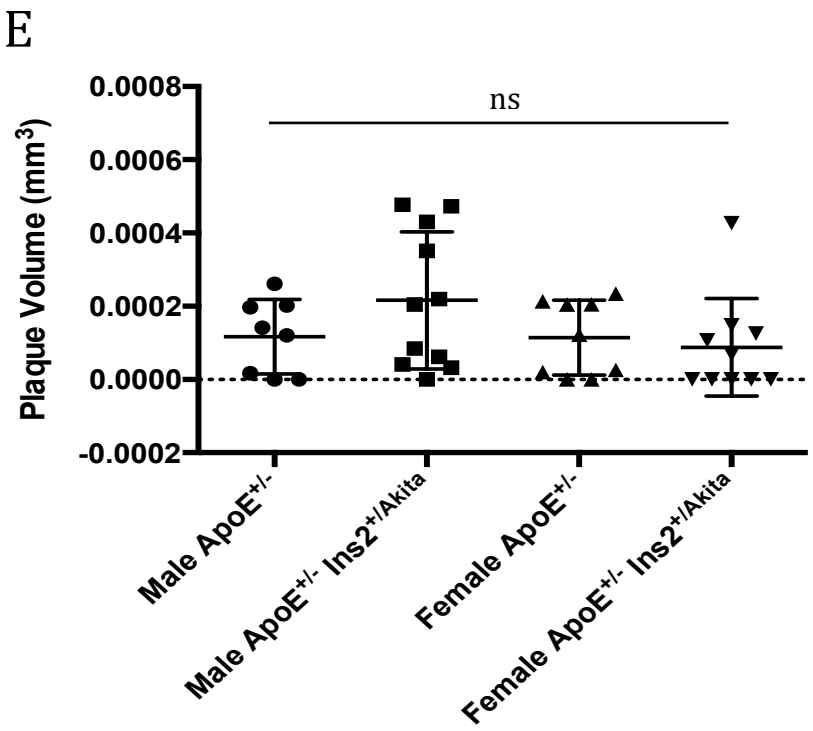

Figure 3: *Plaque Volume of 25-week ApoE$^{+/-}$ mice.* **A-D.** Sample images of aortic sinus cross-sections stained with Mason's Trichrome, where first leaflet is visible: **A.** Male ApoE$^{+/-}$ Ins2$^{+/Akita}$ **B.** Male ApoE$^{+/-}$ **C.** Female ApoE$^{+/-}$ **D.** Female ApoE$^{+/-}$ Ins2$^{+/Akita}$. Lesions are indicated with red arrows. **E.** Quantification of total plaque volume of male and female ApoE$^{+/-}$ and ApoE$^{+/-}$ Ins2$^{+/Akita}$ mice at 25 weeks of age. There were no significant differences between any group (n=7, 11, 9, 9; left to right).

A)

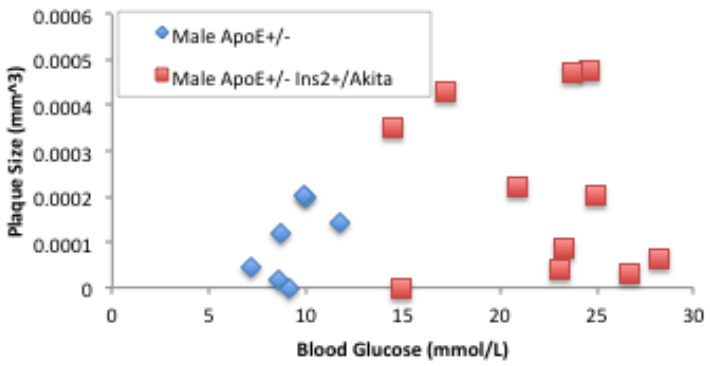

B)

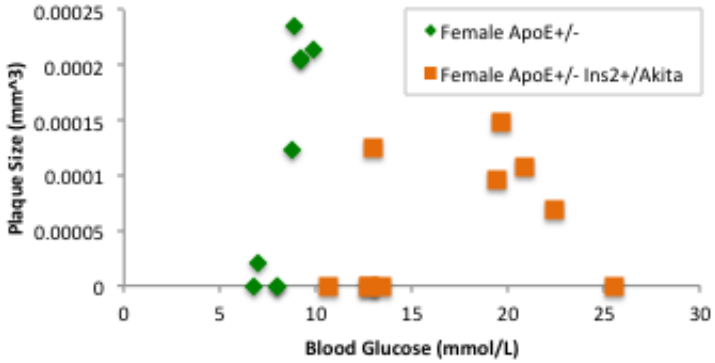

Figure 4: *Blood Glucose and Plaque Volume in 25-week ApoE$^{+/-}$ Mice.* Comparison of plaque volume and blood glucose levels between **A.** male and **B.** female ApoE$^{+/-}$ Ins2$^{+/Akita}$ and ApoE$^{+/-}$ groups. There were no significant correlations.

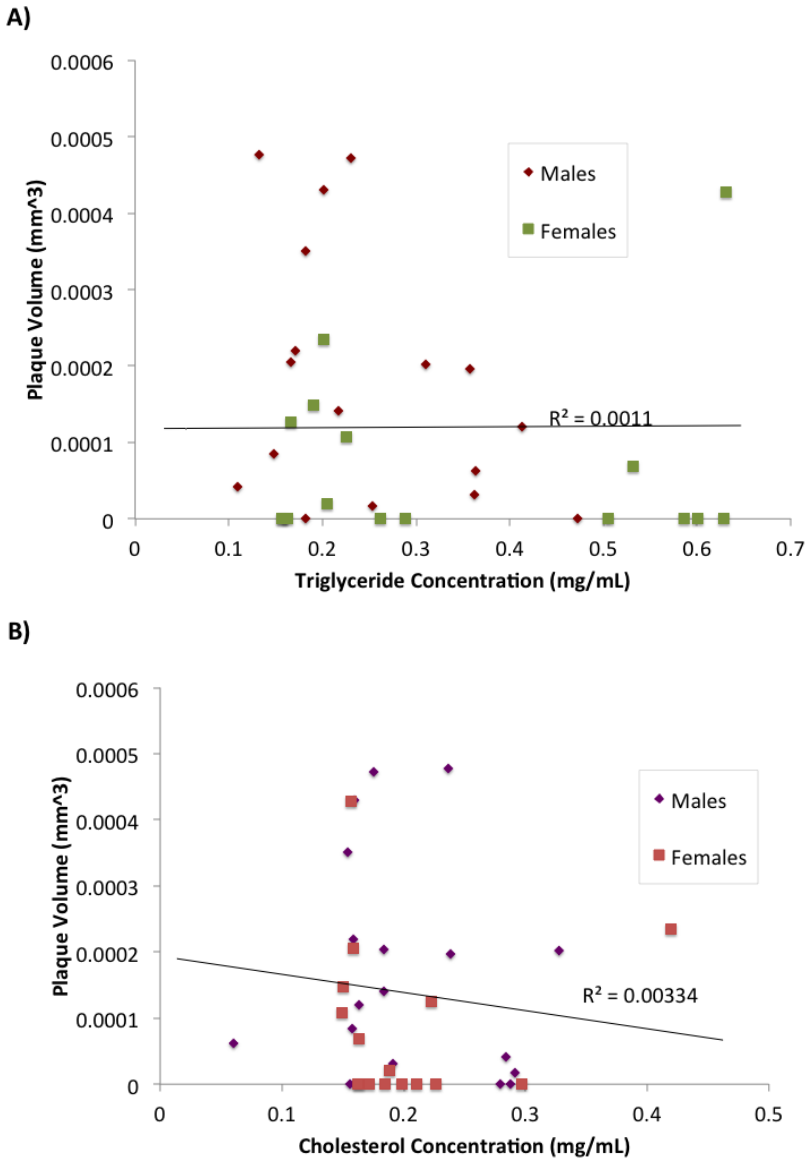

Figure 5: *Triglycerides, Cholesterol, and Plaque Volume in 25-week ApoE$^{+/-}$ Mice.* **A.** Comparison of plaque volume and plasma triglyceride levels (n=17,15) and **B.** Comparison of plaque volume and plasma cholesterol levels (n=17,15). There were no significant correlations.

Discussion

Previous experimental evidence within the Werstuck lab suggested that that $ApoE^{+/-}$ mice may develop plaques when subjected to hyperglycemia (Venegas-Pino et al. 2016), but this was not the case. Neither male nor female $ApoE^{+/-}$ $Ins2^{+/Akita}$ mice demonstrated any significant differences in plaque volume even at 25 weeks (Figure 3e) and the plaques formed were ten times smaller in 25-week old $ApoE^{+/-}$ mice than 10-week old $ApoE^{-/-}$ mice (Figure 8a) (Maeda, 2011). These results suggest that dyslipidemia is a key factor in hyperglycemia-associated atherosclerotic progression (Maeda, 2011; Venegas-Pino et al. 2016).

The first sets of mice were sectioned using a technique that was established for characterization of $ApoE^{-/-}$ mice (with larger plaques) (Venegas-Pino et al. 2013; Venegas-Pino et al. 2016). Hearts were sectioned until the first leaflet was visible and then reoriented until at least one more leaflet was also visible (Braun et al. 2003). This method is intended to reduce the number of slides and sections necessary to complete the sectioning and keep the aortic sinuses in a similar plane of reference (Venegas-Pino et al. 2013). The reorientation often resulted in one or two lost sections at the start, often obscuring the first leaflet (Venegas-Pino et al. 2013). Since the plaques in this model are very small and located near the beginning of the leaflets, the lost sections could result in lost plaques (Venegas-Pino et al. 2013).

To correct this, we adjusted our methods for the second set of $ApoE^{+/-}$ and $ApoE^{+/-}$ $Ins2^{+/Akita}$ mice (Venegas-Pino et al. 2013; Venegas-Pino et al. 2016). The second set was trimmed only until the first leaflet was observed (Braun et al. 2003; Venegas-Pino et al. 2013). The sinus was then sectioned until the final leaflet disappeared (Braun et al. 2003;

Venegas-Pino et al. 2013). To best compare with the first set of mice, the starting point to measure distance was held constant (Venegas-Pino et al. 2013). This new method of sectioning yielded a greater quantity of early sections, containing the beginnings of leaflets where plaques are most likely to form in mice (Braun et al. 2003; Maeda, 2011; Venegas-Pino et al. 2013; Venegas-Pino et al. 2016). Examination of additional mice using this technique revealed some plaque trends that the original method didn't show in the first 24 mice, however overall conclusions remained the same, with no significant differences in atherosclerotic plaque volume between $ApoE^{+/-}$ and $ApoE^{+/-}$ $Ins2^{+/Akita}$ mice in males or females (Figure 3).

$ApoE^{+/-}$ $Ins2^{+/Akita}$ females presented plaque volumes more similar to female $ApoE^{+/-}$ than the male $ApoE^{+/-}$ $Ins2^{+/Akita}$ to male $ApoE^{+/-}$. Our lab has observed evidence of gluconormalization in female $ApoE^{-/-}$ mouse models after 15 weeks (Venegas-Pino et al. 2016). Estrogen has demonstrated anti-apoptotic activity in the beta cells of the murine pancreas (Venegas-Pino et al. 2016), which increases availability of insulin and protects against hyperglycemia (Venegas-Pino et al. 2016); however, in this study, the female Akita mice had significantly elevated blood glucose relative to female controls ($P=0.0168$), even at 25 weeks. While it is possible that genetic drift or stress-related factors could have reduced gluconormalizing effects, previous studies have shown normalizing effects only in female $ApoE^{-/-}$ mice (Maeda, 2011; Venegas-Pino et al. 2016). It would appear that the $ApoE^{+}$ allele in the heterozygote must be responsible for the lack of gluconormalization in the $Ins2^{+/Akita}$ females (Venegas-Pino et al. 2016).

Lipid analyses showed no significant differences in the levels of cholesterol or triglycerides between $ApoE^{+/-}$ $Ins2^{+/Akita}$ mice and the $ApoE^{+/-}$ controls (Figure 2). The

similarity in lipid concentrations suggests that we can exclude these factors as a potential source of the differences between the groups and also reinforces the notion that hyperglycemia is the cause of whatever differences are observed (Maeda, 2011; Shimomura et al. 1999). However, plaque volume and blood glucose did not demonstrate any significant correlations (Figure 4), nor did plaque volume and cholesterol or triglyceride concentrations (Figure 5) in the $ApoE^{+/-}$ mouse model.

Since there were no significant differences in plaque volume between $ApoE^{+/-}$ and $ApoE^{+/-}$ $Ins2^{+/Akita}$ mice, our study looked into the effects of hyperglycemia on the development of atherosclerosis in the endothelium in $ApoE^{-/-}$ mouse model. As expected, both female and male $ApoE^{-/-}$ $Ins2^{+/Akita}$ mice demonstrated hyperglycemia at 10 weeks of age (Figure 7) (Maeda, 2011; Shea et al. 2004; Venegas-Pino et al. 2016). Male $ApoE^{-/-}$ $Ins2^{+/Akita}$ mice demonstrated greater differences in blood glucose relative to controls than female $ApoE^{-/-}$ $Ins2^{+/Akita}$ mice even at 10 weeks of age (Figure 7) ($p<0.0001$ and $p=0.0019$ respectively) (n=8-9). Early activities of these gluconormalizing effects previously described in female ApoE-/- mice are likely the cause of these sex differences (Venegas-Pino et al. 2016). Male $ApoE^{-/-}$ mice were selected as the focus of this study because male $ApoE^{-/-}$ $Ins2^{+/Akita}$ mice expressed the most reliable and pronounced hyperglycemia at 5, 10, 15, and 25 weeks. The fasting blood glucose of the $ApoE^{-/-}$ $Ins2^{+/Akita}$ mice was significantly elevated from their normoglycemic $ApoE^{-/-}$ counterparts ($p=0.0002$, 0.0002, 0.0022, and 0.0079 respectively) (n=5-8) (Figure 6a).

$ApoE^{-/-}$ mice demonstrated plaques averaging ten times larger than $ApoE^{+/-}$ mice and presented at least some plaque in all specimens ($p=0.0021$) (n=16,38) (Figure 8a). This

further supports evidence of the importance of dyslipidemia in the progression of atherosclerosis in mice.

It should be noted that while our lab has previously demonstrated that the $ApoE^{+/-}$ mouse model has normal lipid levels, the results of the lipid analyses in this study were lower than would be expected for all specimens (Maeda, 2011; Venegas-Pino et al. 2016; Zhang et al. 1992). While $ApoE^{-/-}$ plasma cholesterol and triglycerides were within ranges established in other papers, these values for the $ApoE^{+/-}$ mouse model were much lower than should be expected (Falk, 2006; Maeda, 2011; Shea et al. 2004; Venegas-Pino et al. 2016). Similarly, unexpected, the female mice showed significantly elevated fasting plasma triglycerides when the mice were hyperglycemic (Falk, 2006; Maeda, 2011; Venegas-Pino et al. 2016). While these results were suspect and a reassessment was attempted, the reassessment produced similar results and the remaining blood samples were exhausted. Without additional blood samples from 25-week heterozygotes to further assess plasma lipids and with the conclusions of our quantification of plaque volume showing no significant differences in between $ApoE^{+/-}$ and $ApoE^{+/-}$ $Ins2^{+/Akita}$ this study shifted focus to the $ApoE^{-/-}$ model and endothelial activation.

Conclusion

$ApoE^{+/-}$ $Ins2^{+/Akita}$ mice had significantly elevated blood glucose and no differences in plasma cholesterol compared to age-matched controls. There were no significant differences in plaque volume between $ApoE^{+/-}$ and $ApoE^{+/-}$ $Ins2^{+/Akita}$ mice. Hyperglycemia, in normolipidemic mice, is not sufficient to induce the accelerated atherosclerosis.

Chapter 4: Hyperglycemia and Endothelial Activation

Foreword

This study investigates the effects of hyperglycemia on endothelial activation by quantifying the expression of two common markers expressed on the endothelial surface, VCAM and ICAM. It also looks at subsequent macrophage recruitment to these sites prior to plaque formation, and plaque volume over time. We showed here that hyperglycemic mice express more VCAM but not ICAM along their aortic endothelium at as early as 5 and 10 weeks of age and that macrophage recruitment is also increased in hyperglycemic mice at 5 weeks.

Abstract

Objective

Studies of the endothelium and plasma at later stages of atherosclerotic development show a significant rise in both circulating and endothelial VCAM and ICAM especially in mice and patients with chronic hyperglycemia. This study investigates the effects of hyperglycemia on early atherosclerotic development by looking at the markers of endothelial activation and macrophage recruitment to the subendothelial space of the aortic sinus and ascending aorta.

Approach and Results

Blood glucose was measured with a glucometer for each mouse and cholesterol and triglycerides levels were discerned from blood samples treated with infinity reagent chromogens and quantification with absorption chromatography. Hearts of $ApoE^{-/-}$ mice were cut parallel to and 5mm below the aortic sinus and encased in paraffin blocks. These blocks were sectioned and the sections stained with either indirect immunofluorescent

tagging of VCAM or Mac3, to visualize endothelial VCAM expression and macrophage recruitment respectively, or indirect immunohistochemical streptavidinated HRP-DAB staining to visualize endothelial ICAM. Stained sections were imaged at 10x magnification, quantified with ImageJ tracing software, and the percentage of the endothelium expressing VCAM or ICAM was calculated. Mac3 was quantified by measuring the total area of the fluorescent macrophages stained for each mouse. These quantities were compared between age groups, between $ApoE^{-/-}$ and $ApoE^{-/-}$ $Ins2^{+/Akita}$, and between $ApoE^{+/-}$ and $ApoE^{+/-}$ $Ins2^{+/Akita}$ statistically with Man-Whitney *U* tests and Kruskal Wallace *H* tests if they failed the D'Agostino-Pearson omnibus normality test, or Student's *T* tests and One-way ANOVA if they were normally distributed.

Conclusions

This study shows that hyperglycemia increases early VCAM but not ICAM expression in $ApoE^{-/-}$ mice; macrophage recruitment to the subendothelial space is also enhanced in hyperglycemic mice; and hyperglycemic mice develop larger plaques that become evident at 25 weeks of age. These findings are consistent with evidence that VCAM functions as an important endothelial recruitment factor that plays a unique role in the acceleration of atherosclerosis by hyperglycemia. These results further our insight into the mechanisms behind hyperglycemia, its affect on plaque formation, and highlight the importance of VCAM in early macrophage recruitment and atherosclerotic progression independent of ICAM.

Introduction

Atherosclerosis is the most prominent underlying cause of coronary artery disease, carotid artery disease, and peripheral arterial disease (Basta et al. 2004). Atherosclerosis is an immunoinflammatory disease of the medium and large arteries caused by the gradual deposition of lipids and macrophages in the subendothelial space of the arterial wall (Basta et al. 2004). Atheroprone regions; typically, those with turbulent blood flow, branching, or oscillating sheer stress; accumulate excess cholesterol in the form of chylomicrons, VLDL, and LDL in the subendothelial space, which oxidizes and facilitates the chronic inflammation characteristic of the disease (Basta et al. 2004). The endothelium in these lesion-prone areas becomes dysfunctional and activated, expressing cellular adhesion molecules like VCAM and ICAM (Sud et al. 1984). It also becomes more permeable to the very lipids it intends to address (Basta et al. 2004). VCAM and ICAM are adhesion molecules of the immunoglobin (Ig) superfamily expressed along the vascular endothelium and recruit macrophages to clear the lipids and oxidized derivatives from the subendothelial space (Basta et al. 2004; Sud et al. 1984). These macrophages can quickly saturate with lipids, become engorged, and become proatherogenic foam cells (Basta et al. 2004; Blankenberg et al. 2003). Foam cells are fat-engorged M2 macrophages and key actors in lesion formation in nascent atherosclerosis (Venegas-Pino et al. 2016; Walpola et al. 1995). They accumulate in the subendothelial space to become fatty streaks and eventually lesions and advanced plaques (Blankenberg et al. 2003; Venegas-Pino et al. 2016). Research examining this recruitment has shown promising evidence for potential targets of prophylactic intervention (Blankenberg et al. 2003; Cybulsky et al. 2001).

Work by Cybulsky et al. has found evidence that both VCAM and ICAM are upregulated in cases of atherosclerosis in the aorta, however VCAM, but not ICAM, play a large role in lesion initiation (Cybulsky et al. 2001). The study disrupted the fourth immunoglobin (Ig) domain of VCAM or ICAM so that only 2-8% of what is normally produced in the wild type was present (Cybulsky et al. 2001). They found that compromising VCAM significantly reduced the area of early atherosclerotic lesions in $ApoE^{-/-}$ mice, while their plasma lipid profiles, cholesterol, or circulating leukocytes remained comparable to the wild-type (Cybulsky et al. 2001). Conversely, deficiency of ICAM showed no significant changes in plaque initiation or development (Cybulsky et al. 2001).

This is of particular interest to research regarding diabetes (Aronson & Rayfield, 2002; Blankenberg et al. 2003). Chronic hyperglycemia is a hallmark of diabetes and a potent stimulus for inflammation (Aronson & Rayfield, 2002). It should be no surprise that atherosclerosis, a disease characterized by chronic inflammation, is exacerbated by these circumstances (Blankenberg et al. 2003). This synergistic effect leads to significant rises in macrophage recruiting factors and is suspected to be the mechanism behind early initiation and acceleration of cardiovascular disease (Blankenberg et al. 2003; Cybulsky et al. 2001; Venegas-Pino et al. 2016; Walpola et al. 1995).

This study intends to examine the effects of hyperglycemia on the expression and coverage of these macrophage recruitment factors along the aortic sinus endothelium, assess the role of VCAM and ICAM in early atherosclerosis, and look at macrophage recruitment at these nascent stages of atherogenesis in the murine aortic sinus (Blankenberg et al. 2003; Venegas-Pino et al. 2016).

Methods

Harvesting and Sectioning

All ApoE$^{+/-}$ mice were fed a normal chow diet and harvested at 25 weeks of age (Venegas-Pino et al. 2013; Venegas-Pino et al. 2016). ApoE$^{-/-}$ mice were fed a normal chow diet and harvested at 5, 10, 15, and 25 weeks of age (Venegas-Pino et al. 2016). Hearts were perfused with phosphate buffered saline (PBS), harvested, fixed in 10% formalin, processed in a tissue processor, and encased in paraffin blocks (Venegas-Pino et al. 2013). The paraffin-encased tissue was trimmed at 10 micrometers until initial signs of the first leaflet of the aortic valve were observed (Venegas-Pino et al. 2013). The block was then reoriented until the second leaflet became apparent (Venegas-Pino et al. 2013). When at least two of the three aortic valve pouches were visible, the microtome was then switched to section at 4.5 micrometers and sections were fixed to slides via a hot water bath, set to 45 degrees Celsius (Venegas-Pino et al. 2013). Sections were distributed over 10 slides in staggered order (slide 1, slide 2… slide 10, slide 1…) running left to right and top to bottom (Venegas-Pino et al. 2013). Sections were taken until the aortic valve pouches were no longer observed (Venegas-Pino et al. 2013). Due to the small size of plaques in ApoE$^{+/-}$ specimens, this technique was adapted with the second batch of mice so that sectioning would begin at the appearance of the first aortic valve pouch and no reorientation would occur (Venegas-Pino et al. 2013; Venegas-Pino et al. 2016). This was an attempt at reducing the likelihood of missing plaques (Venegas-Pino et al. 2016). Conversely, ApoE$^{-/-}$ hearts were all sectioned until at least 2 aortic valve pouches were visible, as described above (Venegas-Pino et al. 2013).

Quantifying Endothelial Activation

To evaluate endothelial activation, $ApoE^{+/-}$, $ApoE^{+/-}$ $Ins2^{+/Akita}$, $ApoE^{-/-}$, and $ApoE^{-/-}$ $Ins2^{+/Akita}$ hearts were subjected to histochemical (HC) (Venegas-Pino et al. 2016), immunohistochemical (IHC) (Moore et al. 2013; Ruifrok & Johnston, 2001), and immunofluorescent (IF) (Cybulsky et al. 2001; Moore et al. 2013) staining. ICAM was quantified with IHC, using diaminobenzene (DAB) as a chromogen in conjunction with streptavidinated horseradish peroxidase, localized through streptavidin adhesion to a biotinylated secondary antibody, which in turn adhered to a primary antibody specific for ICAM (Ruifrok & Johnston, 2001). Finally, VCAM expression was analyzed via indirect IF tagging of a primary anti-VCAM antibody with a secondary Alexa Fluor 488 fluorescent antibody (Cybulsky et al. 2001; Moore et al. 2013).

ICAM expression was visualized with indirect IHC staining (Cybulsky et al. 2001; Ruifrok & Johnston, 2001). Slides were deparaffinized and treated with citrate-based antigen unmasking solution in a pressure cooker for heat-induced epitope retrieval (HIER) (Moore et al. 2013; Venegas-Pino et al. 2016). Sections were treated with 10% rabbit serum as a blocking agent, diluted in 1X PBS 0.05% triton for permeabilization, for 45 minutes at room temperature (RT) (Moore et al. 2013; Venegas-Pino et al. 2016). Sections were covered with 200uL of goat anti-ICAM-1, an antibody specific for mouse ICAM-1 with biotin affinity, diluted 1:50 in 1X PBS 0.05% triton, and incubated at 4°C overnight (Moore et al. 2013; Venegas-Pino et al. 2016). Slides were washed in 1X PBS and rinsed over 20 minutes and covered with 200uL of a biotinylated rabbit anti-goat secondary antibody, diluted 1:250 in PBS, and incubated for 1.5 hours at RT (Moore et al. 2013; Venegas-Pino et al. 2016). Slides were washed in 1X PBS and covered with streptavidinated horseradish

peroxidase for 45 minutes at RT (Moore et al. 2013; Venegas-Pino et al. 2016). Slides were washed in 1X PBS and treated with DAB for 30 minutes at RT (Moore et al. 2013; Venegas-Pino et al. 2016). They were washed with 1X PBS and mounted with aqueous mounting medium (Moore et al. 2013; Venegas-Pino et al. 2016). Experimental controls were incorporated, which omitted the primary antibody to visualize any nonspecific staining (Moore et al. 2013; Venegas-Pino et al. 2016). Slides were imaged and quantified with colour deconvolution, tracing, and particle analysis using ImageJ software (Venegas-Pino et al. 2013; Venegas-Pino et al. 2016).

VCAM expression was visualized with indirect IF tagging (Cybulsky et al. 2001; Moore et al. 2013). Slides were deparaffinized and treated with citrate-based antigen unmasking solution in a pressure cooker for heat-induced epitope retrieval (HIER) (Moore et al. 2013; Venegas-Pino et al. 2016). Sections were treated with 10% goat serum as a blocking agent, diluted in 1X PBS 0.05% triton for permeabilization, for 45 minutes at room temperature (RT) (Moore et al. 2013; Venegas-Pino et al. 2016). Sections were covered with 200uL of rabbit anti-VCAM-1, diluted 1:50 in 1X PBS 0.05% triton, and incubated at 4°C overnight (Moore et al. 2013; Venegas-Pino et al. 2016). Slides were washed in 1X PBS, rinsed over 20 minutes, and covered with 200uL of fluorescent goat anti-rabbit Alexa Fluor 488 secondary antibody, diluted 1:250 in 1X PBS, and incubated for 1.5 hours at RT (Moore et al. 2013; Venegas-Pino et al. 2016). These slides were protected from exposure to light (Venegas-Pino et al. 2013; Venegas-Pino et al. 2016) (Cybulsky et al. 2001; Moore et al. 2013). Slides were washed with 1X PBS and mounted with aqueous mounting medium (Venegas-Pino et al. 2016). Controls were incorporated, which either omitted the primary antibody or substituted non-specific rabbit IgG. Slides

were imaged, analyzed, and quantified using ImageJ software (Venegas-Pino et al. 2013; Venegas-Pino et al. 2016).

The coverage of VCAM and ICAM expression along the endothelium of the aortic valve pouches was quantified digitally using the tracing tool of ImageJ and standardized with scale bars (Venegas-Pino et al. 2013; Venegas-Pino et al. 2016). This study attempted to account for variation in sizes of aortic sinuses between mice by calculating the percentage of endothelium expressing either VCAM or ICAM (Venegas-Pino et al. 2013; Venegas-Pino et al. 2016). Calculation divided the length of the endothelium expressing either VCAM or ICAM was by the total length of the endothelium in each valve pouch aortic sinus. Sections of the endothelium of aortic sinus valve pouches with excessive non-specific staining were omitted. This was done for all age groups (5, 10, 15, and 25 weeks) and genotypes ($ApoE^{-/-}$, $ApoE^{+/-}$, $ApoE^{-/-}$ $Ins2^{+/Akita}$, and $ApoE^{+/-}$ $Ins2^{+/Akita}$) (Venegas-Pino et al. 2016).

VCAM intensity was not normally distributed and thus was compared with Mann-Whitney *U* tests at 5, 10, 15, and 25-week timepoints (D'Agostino et al. 1990). Once considered within age groups and gender, these analyses were also performed via Kruskal-Wallis *H* tests to run multiple comparisons between the groups (McKnight & Najab, 2010).

Groups were tested for normal distribution with D'Agostino & Pearson omnibus normality tests (D'Agostino et al. 1990). Small sample sizes ($n<8$) often give false positives for normality tests (D'Agostino et al. 1990; Heiberger & Neuwirth, 2009; McKnight & Najab, 2010). It is more reliable to use non-parametric analyses in these cases (McKnight & Najab, 2010). For this reason, samples that did not present with normal distribution, or had sample sizes below 8, were analyzed with non-parametric analyses (D'Agostino et al.

1990). Comparisons between two groups were analyzed with non-parametric Mann-Whitney *U* tests (D'Agostino et al. 1990). Comparisons between multiple groups were conducted with non-parametric Kruskal-Wallis *H* tests (McKnight & Najab, 2010). Normally distributed data was analyzed with t-tests for comparisons between two groups or one-way ANOVA for multiple comparisons (Haynes, 2013; Heiberger & Neuwirth, 2009).

Results

Metabolic Parameters

Male ApoE$^{-/-}$ Ins2$^{+/Akita}$ mice had significantly elevated blood glucose levels relative to age and sex-matched ApoE$^{-/-}$ controls at 5, 10, 15, and 25 weeks of age (p=0.0002, 0.0002, 0.022, and 0.079 respectively) (n=5-9) (Figure 6a). Female ApoE$^{-/-}$ Ins2$^{+/Akita}$ mice had significantly higher blood glucose than their age matched ApoE$^{-/-}$ counterparts at 10 weeks of age (p=0.0019) (n=9-10) (Figure 7).

Some female ApoE$^{-/-}$ Ins2$^{+/Akita}$ mice had similar or lower blood glucose than their ApoE$^{-/-}$ counterparts (Figure 7). This is consistent with previous studies in our lab, which show that glucose levels normalize in female ApoE$^{-/-}$ mice after sexual maturation[4]. Because we are interested in the effect of hyperglycemia on atherogenesis, this study opted to focus on male mice[4]. Male ApoE$^{-/-}$ Ins2$^{+/Akita}$ mice showed significantly elevated fasting plasma cholesterol at 15 (P=0.0159) and 25 weeks of age (P=0.0079) compared to age-matched ApoE$^{-/-}$ mice (p=0.0159 and 0.0079 respectively) (n=5) (Figure 6b). There were no significant differences in fasting plasma triglycerides between male ApoE$^{+/-}$ Ins2$^{+/Akita}$ and ApoE$^{-/-}$ mice at any age (n=3-5) (Figure 6c).

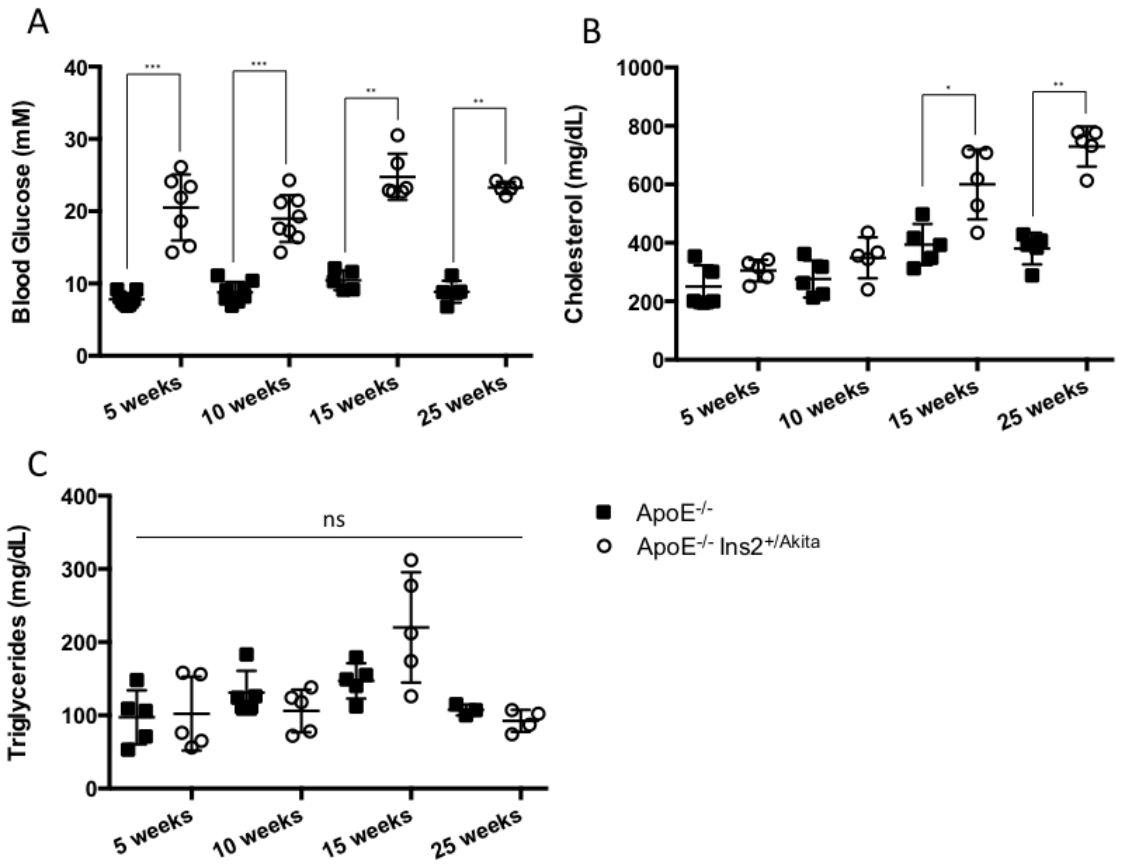

Figure 6. *Analysis of Glucose and Lipid Levels in Male ApoE$^{-/-}$ Mice.* **A.** Male ApoE$^{-/-}$ Ins2$^{+/Akita}$ mice showed significantly higher blood glucose than male ApoE$^{-/-}$ mice at 5, 10, 15, and 25 weeks of age. (p=0.002, 0.002, 0.022, 0.079 respectively) (n=9,7,8,8,5,6,5,5) **B.** Male ApoE$^{-/-}$ Ins2$^{+/Akita}$ mice demonstrated significantly elevated cholesterol at 15 and 25 weeks of age relative to age matched controls. (p=0.0159, 0.0079 respectively) (n=5) **C.** There were no significant differences in triglyceride levels in either genotype at any age examined. (n=5,5,5,5,5,5,3,4)

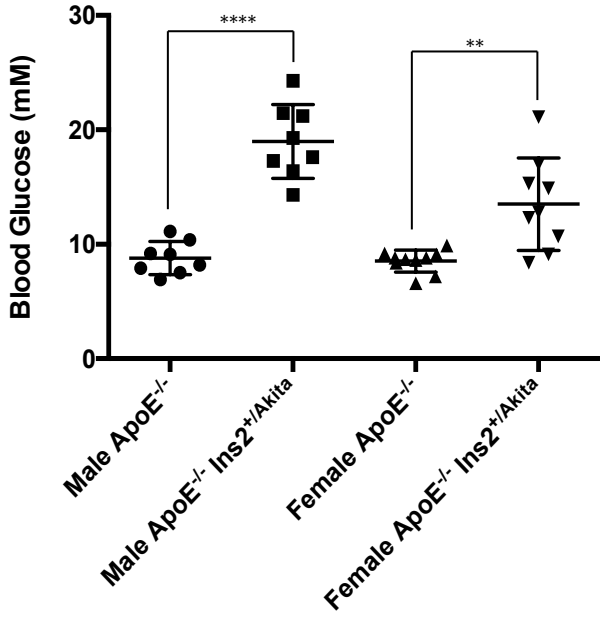

Figure 7: *Blood glucose levels in 10-week ApoE$^{-/-}$ mice*. Male ApoE$^{-/-}$ Ins2$^{+/Akita}$ mice had significantly higher blood glucose than male ApoE$^{-/-}$ ($p<0.0001$) (n=8). Female ApoE$^{-/-}$ Ins2$^{+/Akita}$ mice also had significantly higher blood glucose than female ApoE$^{-/-}$ ($p=0.0019$) (n=10,9). Males demonstrated greater and more reliable differences in blood glucose than females between ApoE$^{-/-}$ and ApoE$^{-/-}$ Ins2$^{+/Akita}$.

Atherosclerotic Plaque Volume

Male ApoE$^{-/-}$ Ins2$^{+/Akita}$ mice at 10 weeks had significantly larger plaques than ApoE$^{+/-}$ mice at 25 weeks ($p<0.0001$) (n=16,38) (Figure 8a). Both male ApoE$^{-/-}$ and ApoE$^{-/-}$ Ins2$^{+/Akita}$ mice presented with distinct and significant plaques by 15 and 25 weeks of age (Figure 8b,c). Male ApoE$^{-/-}$ Ins2$^{+/Akita}$ mice presented significantly larger plaque volume, approximately 3 times larger than male ApoE$^{-/-}$ mice, at 25 weeks of age (Figure 8a) ($p=0.0317$) (n=4-7).

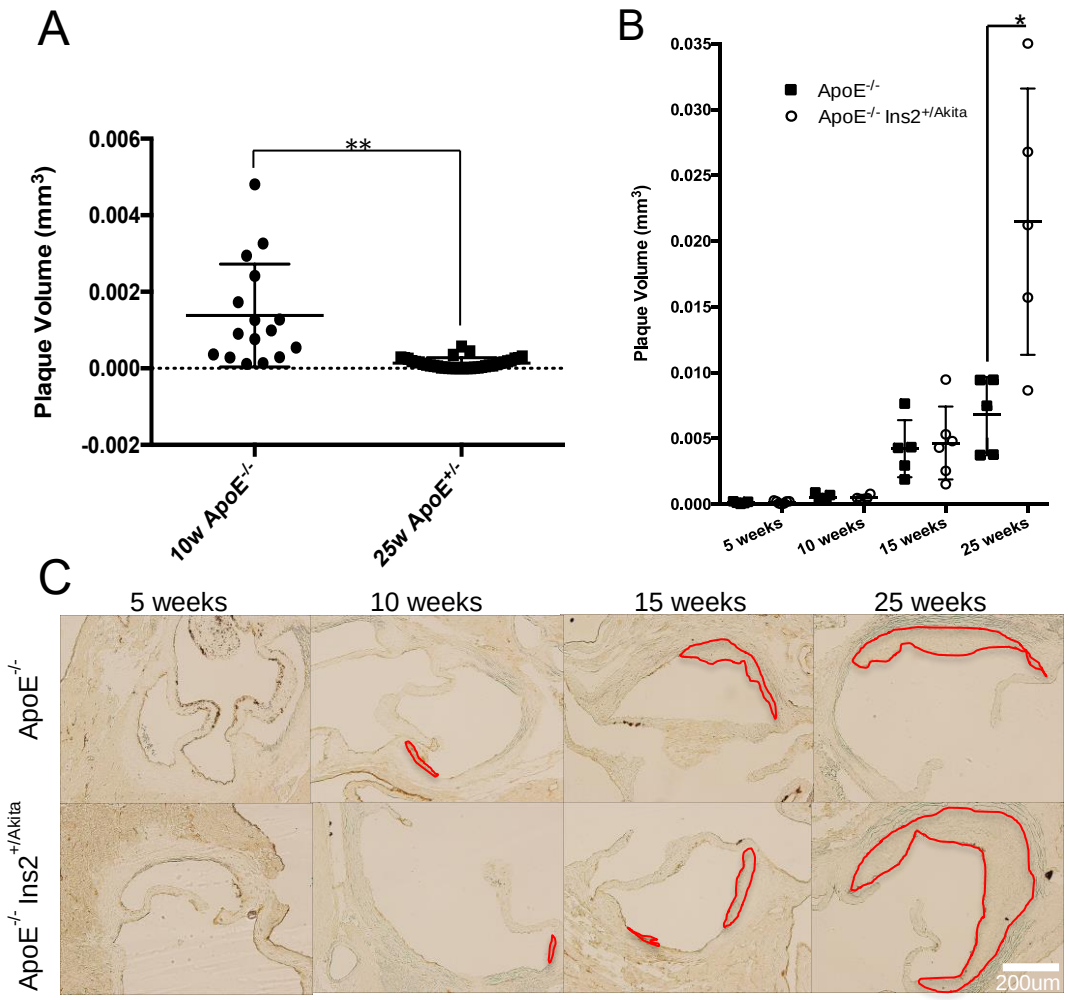

Figure 8: *Plaque Volume of Male ApoE$^{-/-}$ Mice.* A. Quantification of plaque volume in the aortic sinus of 10-week ApoE$^{-/-}$ and 25-week ApoE$^{+/-}$ model mice. Plaques in ApoE$^{-/-}$ model were 10 times larger than ApoE$^{+/-}$ at 25 weeks ($P<0.0001$) (n=16,38). B. Quantification of the plaque area in the aortic sinus at 5, 10, 15, and 25 weeks of age. Plaques presented in both ApoE$^{-/-}$ and ApoE$^{-/-}$ Ins2$^{+/Akita}$ mice at 15 weeks. ApoE$^{-/-}$ Ins2$^{+/Akita}$ mice presented significantly larger plaque size at 25 weeks ($p=0.0317$) (n=5,7,5,4,5,6,5,5). C. Representative sections of aortic root were taken from normoglycemic ApoE$^{-/-}$ and hyperglycemic ApoE$^{-/-}$ Ins2$^{+/Akita}$ mice. Atherosclerotic lesions are outlined in red.

VCAM Expression

Indirect IF staining of male ApoE$^{-/-}$ aortic sinuses showed specific fluorescence along the endothelial lining in sections 0-180um rom the aortic root, indicative of VCAM expression (Figure 9b).

Male ApoE$^{-/-}$ Ins2$^{+/Akita}$ mice expressed elevated levels of VCAM at 5 and 10 weeks of age, compared to their normoglycemic ApoE$^{-/-}$ counterparts (p=0.0079 and 0.0037 respectively) (n=6-9) (Figure 10a). Male ApoE$^{-/-}$ Ins2$^{+/Akita}$ mice showed sustained high levels of endothelial VCAM, with linear regression analysis showing no significant changes from 5 to 25 weeks (p=0.2010) (R^2=0.3588) (n=3-9) (Figure 10c). Conversely, linear regression analysis on male ApoE$^{-/-}$ mice showed a significant increase in VCAM expression over time from 5 to 25 weeks (p=0.0041) (R^2=0.0804) (n=3-8) (Figure 10c).

Examination of VCAM in the ascending aorta, sectioned 319.5-495um from the aortic root, we see no significant differences in VCAM expression between male ApoE$^{-/-}$ and ApoE$^{-/-}$ Ins2$^{+/Akita}$ mice along the endothelium at 5 or 25 weeks of age, however Mann-Whitney *U* tests on both groups show a significant rise in VCAM expression of both male ApoE$^{-/-}$ and ApoE$^{-/-}$ Ins2$^{+/Akita}$ mice between 5 and 25 weeks (p=0.0357 and 0.0238 respectively) (n=3-6) (Figure 11). Quantification of mean grey value showed similar intensity of fluorescent VCAM in male ApoE$^{-/-}$ Ins2$^{+/Akita}$ mice at 10, 15, and 25 weeks (n=3-5) (Figure 12).

ApoE$^{+/-}$ Ins2$^{+/Akita}$ mice demonstrated no significant differences in VCAM expression relative to age and sex-matched controls in sections 0-180um from the aortic root (Figure 13).

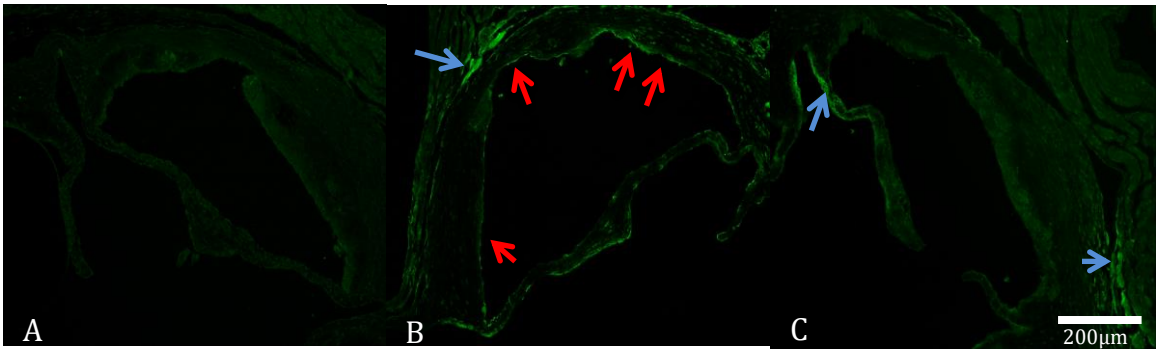

Figure 9: *Sample Images of VCAM Fluorescence.* Sample images of immunofluorescent staining with: **A.** no primary antibody **B.** VCAM-1-specific antibody **C.** and non-specific rabbit IgG. Red arrows indicate regions of specific staining of VCAM along the endothelium. Blue arrows indicate regions of nonspecific staining. There is little to no staining in the staining with no primary antibody; there is specific endothelial staining when using the VCAM antibody with some non- specific staining; and there is non-specific staining when using the rabbit IgG.

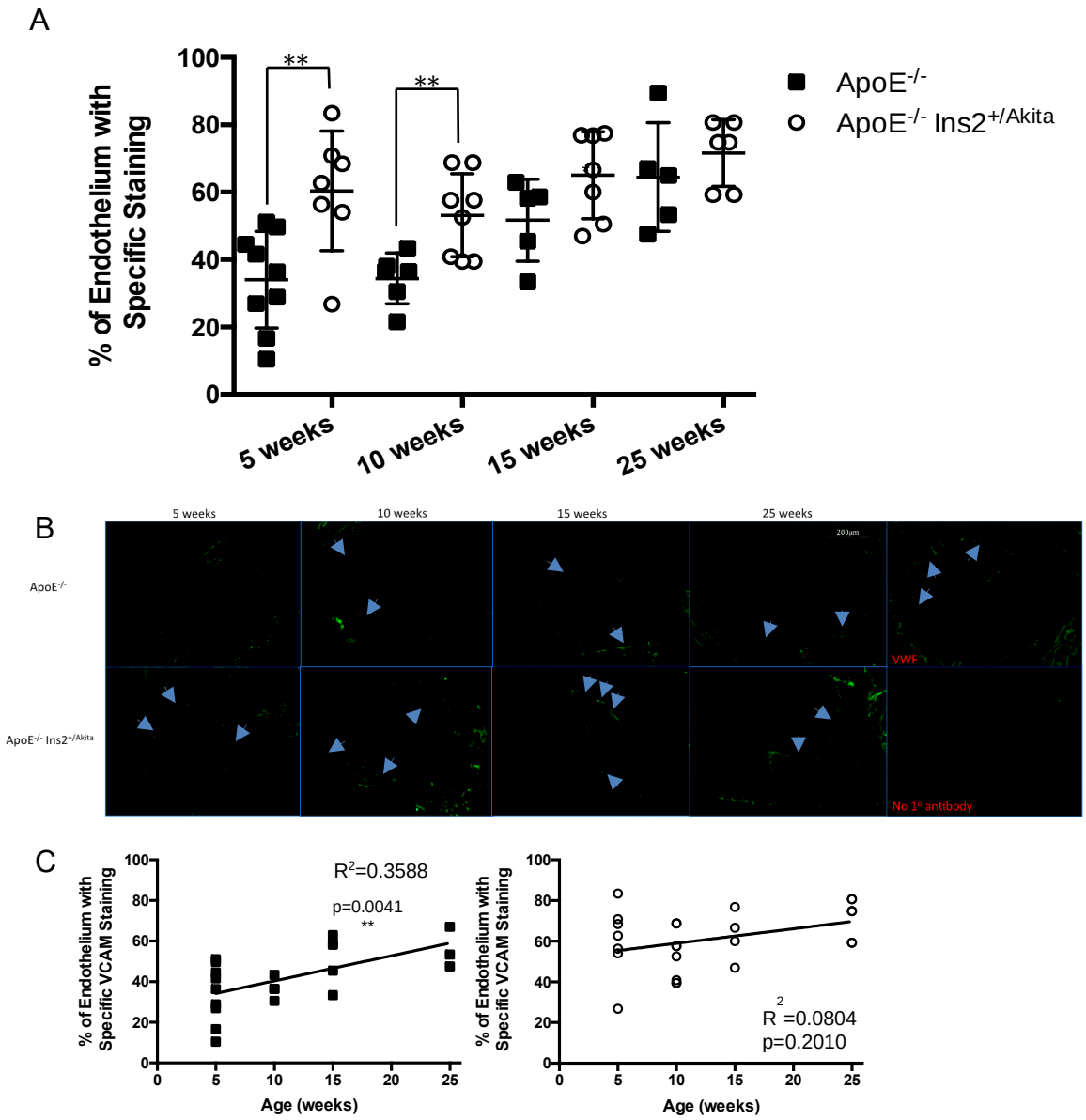

Figure 10. *Endothelial VCAM Expression in ApoE$^{-/-}$ Mice.* **A.** Aortic sinus endothelium expressing VCAM. ApoE$^{-/-}$ Ins2$^{+/Akita}$ mice show higher VCAM expression at 5 (p=0.0079) and 10 (p=0.0037) weeks of age. (n=9,7,6,8,5,7,5,6) **B.** Representative sections of the aortic sinus treated with indirect immunofluorescence at 5, 10, 15, and 25 weeks of age. Specific staining of endothelial VCAM is indicated with blue arrows. VWF was used as a positive control and demonstrated staining of the whole endothelium. Negative controls showed no specific fluorescence. **C.** Linear regression of VCAM coverage in ApoE$^{-/-}$ and ApoE$^{-/-}$ Ins2$^{+/Akita}$ mice over time. ApoE$^{-/-}$ mice show significant rise over time (p=0.0041) (R2=0.3588) (n=9,4,5,3), while ApoE$^{-/-}$ Ins2$^{+/Akita}$ mice show no significant change over time (p=0.2010) (R2=0.0804) (n=7,8,4,3).

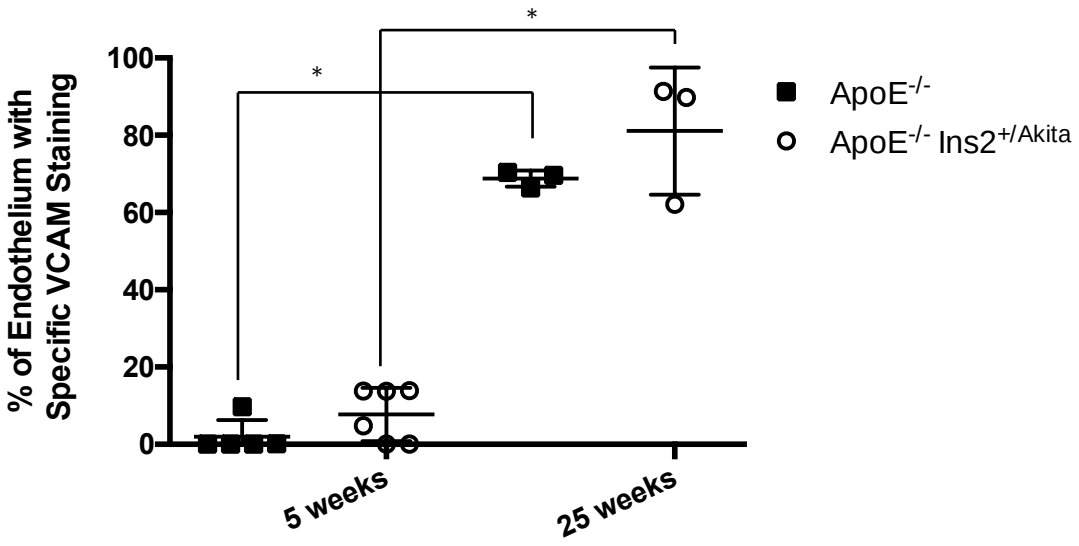

Figure 11: Endothelial VCAM Expression in the Ascending Aorta in ApoE$^{-/-}$ Mice. ApoE$^{-/-}$ Ins2$^{+/Akita}$ mice showed no significant differences in VCAM coverage from ApoE$^{-/-}$ mice at 5 or 25 weeks, however VCAM coverage rose significantly in both groups by 25 weeks ($p=0.0357$ for ApoE$^{-/-}$, 0.0238 for ApoE$^{-/-}$ Ins2$^{+/Akita}$) (n=5,6,3,3).

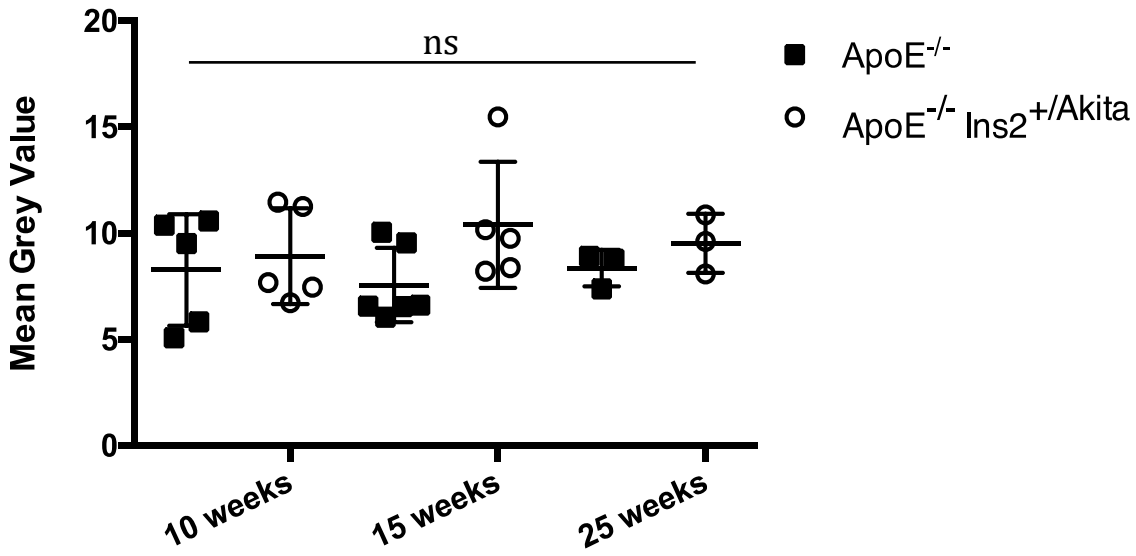

Figure 12: *VCAM Fluorescence Intensity in ApoE$^{-/-}$ Mice.* Average intensity of fluorescence of aortic leaflets in male ApoE$^{-/-}$ and ApoE$^{-/-}$ Ins2$^{+/Akita}$ mice at 10, 15 and 25 weeks (n=5,5,6,5,3,3). While ApoE$^{-/-}$ Ins2$^{+/Akita}$ mice appear to have higher expression at each time-point, there are no significant differences. There is no significant difference in VCAM intensity between 10, 15, and 25-week mice.

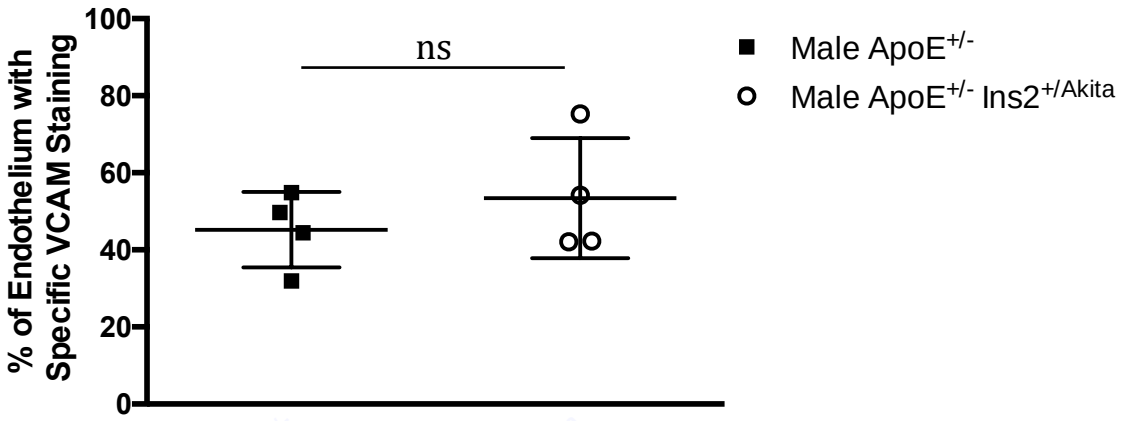

Figure 13: *Endothelial VCAM Expression in ApoE$^{+/-}$ Mice.* Quantification of the percentage of the endothelium expressing fluorescent VCAM in male ApoE$^{+/-}$ and ApoE$^{+/-}$ Ins2$^{+/Akita}$ at 25 weeks. There were no significant differences (n=4).

ICAM Expression

Cross sections of the aortic sinus were stained for ICAM via indirect IHC staining with DAB, streptavidinated horseradish peroxidase and a biotinylated secondary antibody and displayed red oxidized DAB localized along the endothelium, indicative of ICAM-specific staining (Figure 14).

In sections taken 0-180um from the aortic root, male $ApoE^{-/-}$ $Ins2^{+/Akita}$ mice showed no significant differences in ICAM expression relative to age and sex-matched $ApoE^{-/-}$ mice at any age (n=4-8) (Figure 15a). $ApoE^{-/-}$ $Ins2^{+/Akita}$ and $ApoE^{-/-}$ mice showed similar significant increases in the coverage of ICAM along the endothelium over time, increasing gradually but significantly from 5 to 25 weeks or age (p=0.0235 and 0.0438 respectively) (R^2=0.2214 and 0.1722 respectively) (Figure 15c).

In the ascending aorta in sections 319.5-49.5um from the aortic root, there are no significant differences in ICAM expression between $ApoE^{-/-}$ and $ApoE^{-/-}$ $Ins2^{+/Akita}$ mice at 5 or 25 weeks along the endothelium (n=5-7) (Figure 16).

$ApoE^{+/-}$ mice also demonstrated no significant differences in ICAM expression between male 25-week $ApoE^{+/-}$ and $ApoE^{+/-}$ $Ins2^{+/Akita}$ mice in sections from 0-180um deep (n=3) (Figure 17).

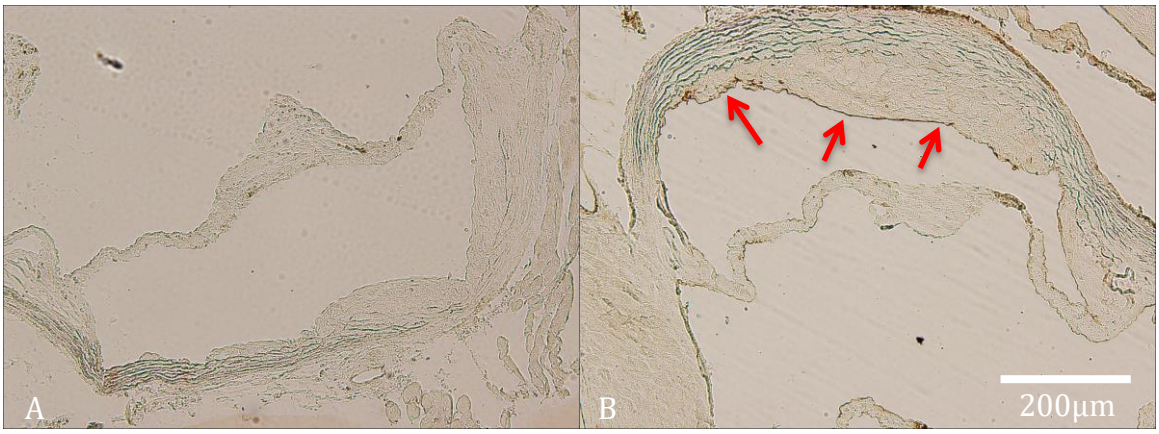

Figure 14: Sample Images of ICAM-specific DAB Staining. Sample images of IHC staining with: **A.** no primary antibody and **B.** ICAM-1-specific antibody. Red arrows indicate regions of specific staining of ICAM along the endothelium. There is no staining when omitting the primary antibody and there is specific endothelial staining when using the ICAM-specific antibody. Both images are of male ApoE$^{-/-}$ Ins2$^{+/Akita}$ mice at 15 weeks.

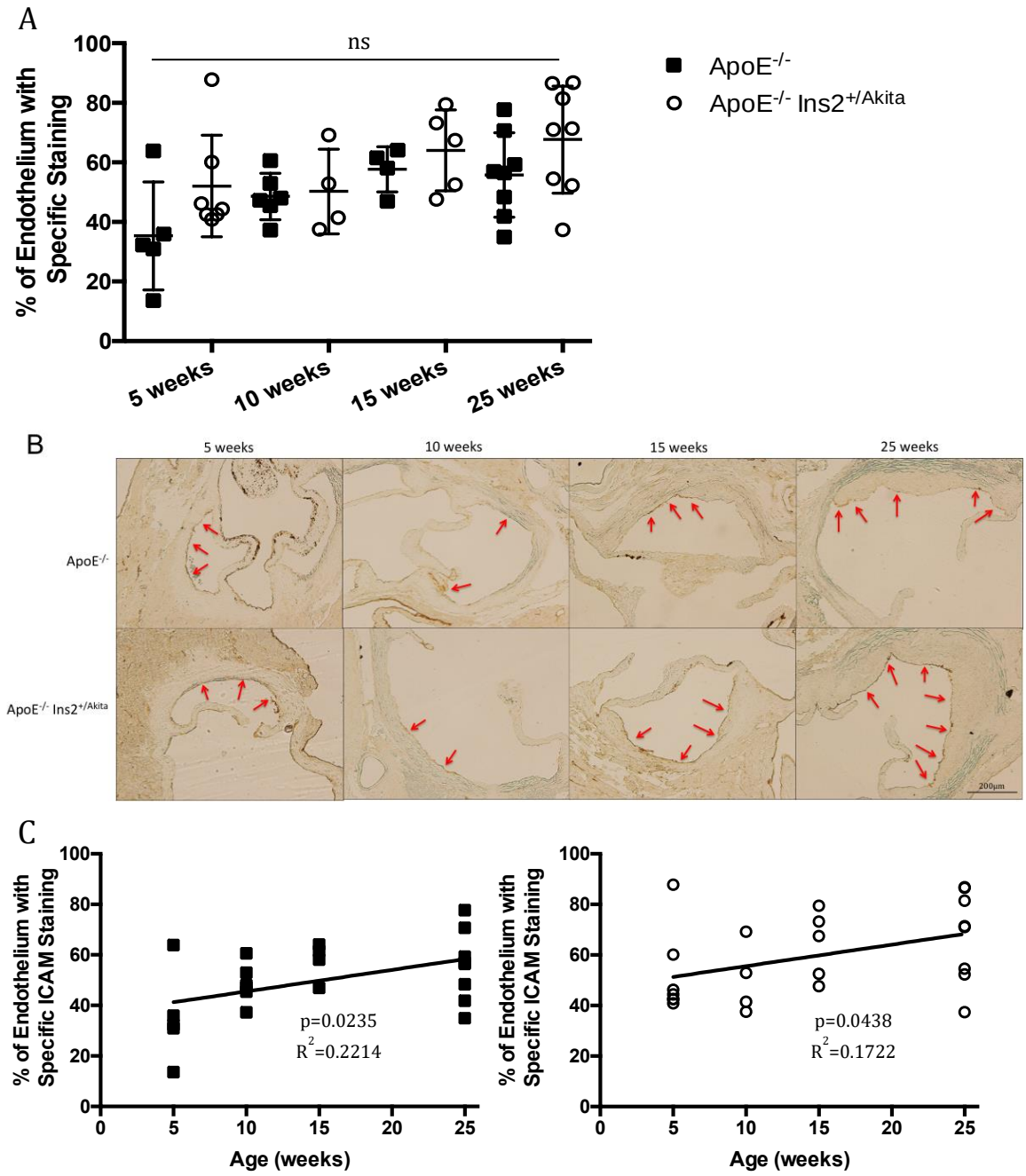

Figure 15. *Endothelial ICAM Expression in ApoE$^{-/-}$ mice.* **A.** Quantification of ICAM expression along the aortic sinus endothelium. No significant differences in ICAM expression between ApoE$^{-/-}$ Ins2$^{+/Akita}$ or ApoE$^{-/-}$ mice at 5, 10, 15, or 25 weeks (n=5,7,6,4,4,5,8,8) **B.** Representative sections of aortic root stained with biotinylated anti-ICAM, streptavidinated horseradish peroxidase, and diaminobenzene. Specific staining of endothelial ICAM indicated with red arrows. C. Linear regression of ICAM coverage in ApoE$^{-/-}$ and ApoE$^{-/-}$ Ins2$^{+/Akita}$ mice over time. ICAM coverage of both ApoE$^{-/-}$ and ApoE$^{-/-}$ Ins2$^{+/Akita}$ mice rose significantly over time (p=0.0235 and 0.0438 respectively) (R2=0.2214 and 0.1722 respectively) (n=5,6,4,8 and 7,4,5,8 respectively).

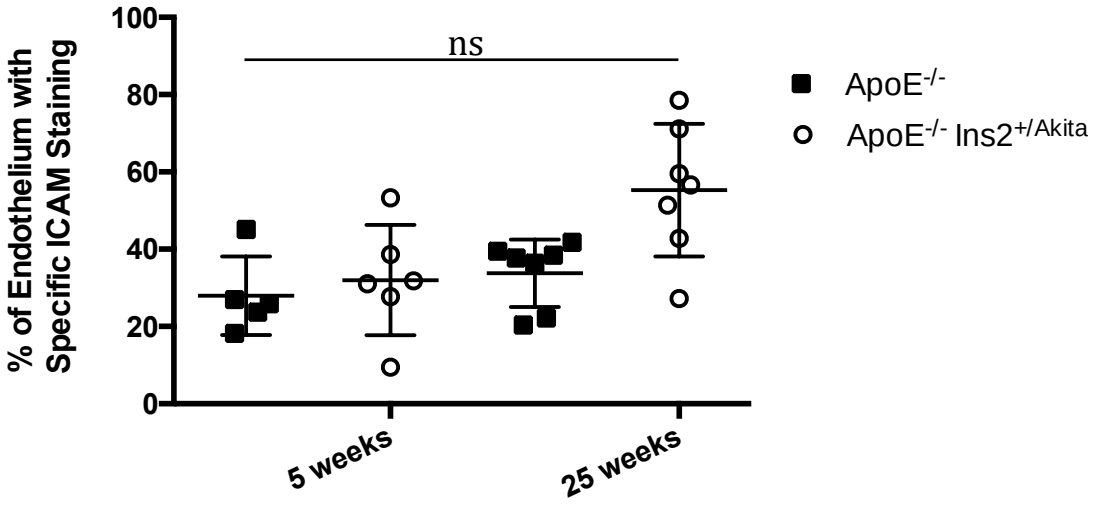

Figure 16. *Endothelial ICAM Expression in the Ascending Aorta of ApoE$^{-/-}$ mice.* Sections of the upper aortic sinus and ascending aorta showed no significant differences in the coverage of ICAM along the endothelium between ApoE$^{-/-}$ and ApoE$^{-/-}$ Ins2$^{+/Akita}$ mice at 5 or 25 weeks (n=5,6,7,7). There was also no significant difference in the endothelial coverage of ICAM between 5 and 25 weeks for either group.

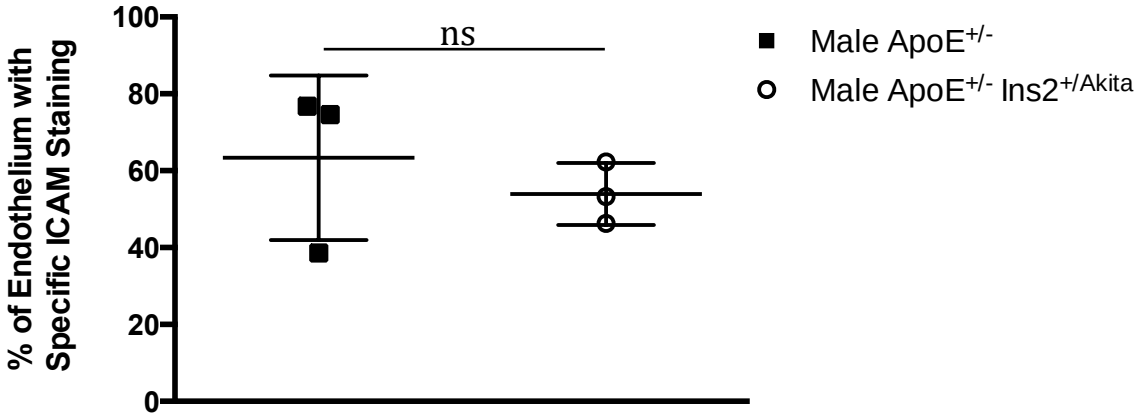

Figure 17: *Endothelial ICAM Expression in ApoE$^{+/-}$ Mice.* Quantification of the percentage of the endothelium expressing DAB-stained ICAM in male ApoE$^{+/-}$ and ApoE$^{+/-}$ Ins2$^{+/Akita}$ at 25 weeks. There were no significant differences (n=3).

Macrophage Recruitment

Aortic sinus sections were immunostained with an antibody against CD-107b (Mac3) using indirect immunofluorescence and demonstrated specific staining along the endothelium and within plaques (Figure 18b). $ApoE^{-/-}$ $Ins2^{+/Akita}$ mice presented significantly greater macrophage recruitment than $ApoE^{-/-}$ at 5 weeks (P=0.0002) (Figure 16a). Macrophage recruitment in $ApoE^{-/-}$ mice rose significantly by 10 weeks to levels similar to what was seen in $ApoE^{-/-}$ $Ins2^{+/Akita}$ at 5 weeks (P=0.0002) (n=7-9).

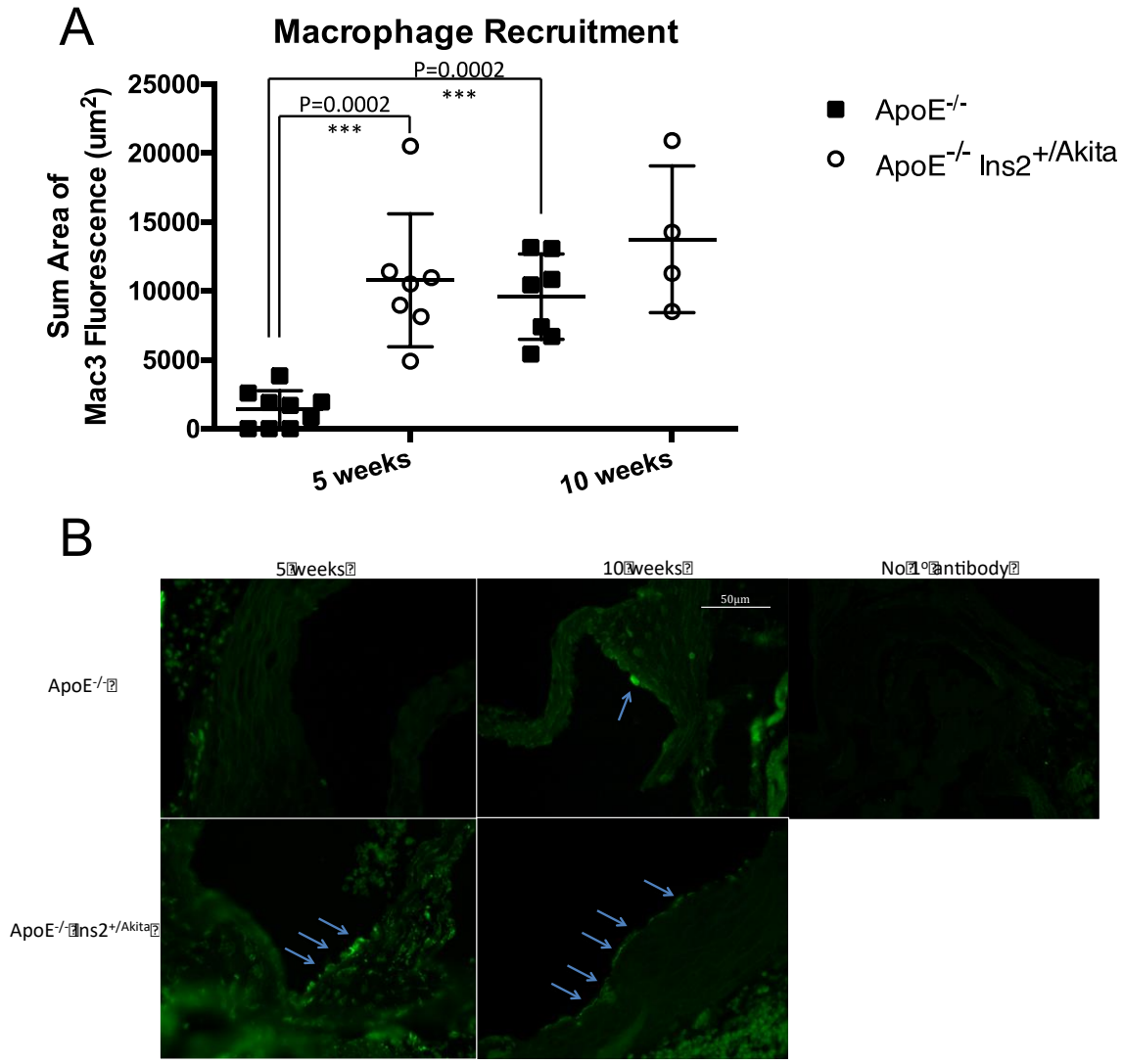

Figure 18. *Macrophage Recruitment in ApoE$^{-/-}$ Mice.* **A.** Quantification of macrophage area measured as a sum of the area of all fluorescent macrophages for each mouse. ApoE$^{-/-}$ Ins2$^{+/Akita}$ mice presented significantly greater macrophage recruitment than ApoE$^{-/-}$. (p=0.0002) (n=9,8,7,4). Macrophage recruitment in ApoE$^{-/-}$ mice rose significantly at 10 weeks to levels similar to ApoE$^{-/-}$ Ins2$^{+/Akita}$ at 5 weeks. (p=0.0002) **B.** Representative sections of the aortic sinus stained with indirect immunofluorescence, specific for Mac3, a marker present on the surface of the target macrophages. Blue arrows indicate specific staining of macrophages along the endothelium and within the subendothelial space. Fluorescent macrophages can be seen at 10 weeks in both ApoE$^{-/-}$ and ApoE$^{-/-}$ Ins2$^{+/Akita}$ mice, however fluorescent macrophages are scarce in ApoE$^{-/-}$ but prevalent in ApoE$^{-/-}$ Ins2$^{+/Akita}$ mice at 5 weeks.

Discussion

Endothelial VCAM Expression

This study looked at endothelial activation in ApoE$^{-/-}$ and ApoE$^{+/-}$ mouse models (Venegas-Pino et al. 2016). IF staining of VCAM using a monoclonal rabbit anti-VCAM-1 antibody showed specific staining that was not observed with rabbit IgG or when omitting the primary antibody (Figure 9) (Moore et al. 2013). This is evidence that the fluorescence localized to the aortic valve pouch endothelium is representative of VCAM expression (Cybulsky et al. 2001; Venegas-Pino et al. 2016). Quantification of the percentage of endothelium expressing fluorescent VCAM found that VCAM expression was significantly elevated in ApoE$^{-/-}$ Ins2$^{+/Akita}$ mice relative to ApoE$^{-/-}$ mice at 5 and 10 weeks of age ($p=0.0079$, 0.0037 respectively) ($n=6$-9) (Figure 10a). This rise in VCAM expression occurs before plaques can be detected (Figure 10b) (Venegas-Pino et al. 2013; Venegas-Pino et al. 2016). ApoE$^{-/-}$ mice typically present plaques, by 15 weeks of age when fed a standard chow diet (Venegas-Pino et al. 2016). In this study, ApoE$^{-/-}$ Ins2$^{+/Akita}$ mice maintain similar elevated VCAM expression at 5, 10, 15, and 25 weeks, while ApoE$^{-/-}$ mice show a more gradual rise to similar levels by 15 or 25 weeks of age (Figure 10c). Linear regression analysis showed the significance of this rise in VCAM expression for ApoE$^{-/-}$ but not ApoE$^{-/-}$ Ins2$^{+/Akita}$ mice ($p=0.0041$ and 0.2010 respectively), however it should be noted that the linear regression for each presented low R^2 values ($R^2=0.3588$ and 0.0804 respectively) and therefore, while the linear regression model for ApoE$^{-/-}$ mice was significant ($p=0.0041$), neither regression model accurately explains the variation in the data (Rousseeuw & Leroy, 2005). Regardless, we see elevated VCAM coverage along the aortic endothelium in ApoE$^{-/-}$ Ins2$^{+/Akita}$ mice with chronic hyperglycemia at 5, 10, 15 and

25 weeks, where ApoE$^{-/-}$ only present similar levels at 15 and 25 weeks (Venegas-Pino et al. 2016). This suggests that hyperglycemia stimulates endothelial activation earlier in ApoE$^{-/-}$ mice (Blankenberg et al. 2003; Ruifrok & Johnston, 2001). Since VCAM expression in ApoE$^{-/-}$ mice does not significantly change between 5 and 25 weeks and VCAM expression in ApoE$^{-/-}$ mice rises to similar levels around 15 and 25 weeks, this may also suggest some maximal threshold of endothelial VCAM expression, which is achieved early on by ApoE$^{-/-}$ Ins2$^{+/Akita}$ mice and which ApoE$^{-/-}$ mice build to more gradually (Cybulsky et al. 2001; Ruifrok & Johnston, 2001). As atherosclerotic plaques progress, macrophages are recruited to the subendothelial space at sites of inflammation by cellular adhesion molecules like VCAM and ICAM (Cybulsky et al. 2001; Ruifrok & Johnston, 2001). Over time, this inflammation becomes more and more severe and macrophages continue to be recruited (Basta et al. 2004). There is no significant difference in VCAM expression in either group between 15 and 25 weeks, where most plaque growth is likely to occur (Basta et al. 2004). Our results seem to support the notion of a maximal threshold of VCAM coverage, which is reached earlier in hyperglycemic ApoE$^{-/-}$ Ins2$^{+/Akita}$ mice than ApoE$^{-/-}$ mice and is realized at 15 and 25 weeks in both groups (Cybulsky et al. 2001).

It should be noted that there was no difference in the intensity of this VCAM fluorescence per unit area between the ApoE$^{-/-}$ and ApoE$^{-/-}$ Ins2$^{+/Akita}$ mice. Instead the quantification of mean gray values showed a uniform intensity of VCAM fluorescence along the endothelium at all ages (Blankenberg et al. 2003). This significant rise in VCAM coverage along the endothelium with no rise in intensity may suggest an all-or-none mechanism of VCAM expression by endothelial cells; where VCAM upregulation does not increase the VCAM produced by individual cells as much as increase the number of

cells expressing VCAM (Cybulsky et al. 2001). This idea is currently under investigation in the Werstuck lab. In either case, it would appear that mice with hyperglycemia display a greater area of the endothelium expressing VCAM but no difference in its intensity per unit area (Cybulsky et al. 2001; Ruifrok & Johnston, 2001; Venegas-Pino et al. 2016).

These results were not mirrored in the male $ApoE^{+/-}$ mouse model, where there were no differences in VCAM coverage between $ApoE^{+/-}$ and $ApoE^{+/-}$ $Ins2^{+/Akita}$ mice (Venegas-Pino et al. 2016). These experiments seem to suggest that hyperglycemia significantly increases area of expression but not essentially intensity of VCAM along the endothelium; and that dyslipidemia, as seen in the $ApoE^{-/-}$ but not $ApoE^{+/-}$ mouse model, plays a key role in increasing the extent of VCAM coverage in these atherosclerosis-susceptible regions of the endothelium (Venegas-Pino et al. 2016).

ICAM Expression

Similarly, to VCAM immunofluorescent experiments, immunohistochemical staining of ICAM using goat anti-ICAM-1 showed a specific staining that was not observed with goat IgG or when omitting the primary antibody (Figure 14) (Cybulsky et al. 2001; Venegas-Pino et al. 2016). This suggests that the localized DAB staining is representative of ICAM expression along the endothelium (Ruifrok & Johnston, 2001). Unlike VCAM, quantification of endothelial ICAM showed no significant differences in coverage between $ApoE^{-/-}$ $Ins2^{+/Akita}$ and $ApoE^{-/-}$ mice (Figure 15). $ApoE^{+/-}$ and $ApoE^{+/-}$ $Ins2^{+/Akita}$ mice also showed no significant differences (Figure 17). Instead, linear regression analysis showed a significant rise in ICAM expression for both $ApoE^{-/-}$ and $ApoE^{-/-}$ $Ins2^{+/Akita}$ mice ($p=0.0235$ and 0.0438 respectively), however, like our previous linear regression in VCAM, it should be noted that the linear regression for each genotype, $ApoE^{-/-}$ and $ApoE^{-/-}$ $Ins2^{+/Akita}$,

presented low R^2 values (R^2=0.2214 and 0.1722 respectively) and therefore, while both analyses are significant, they do not explain the variation in the data accurately.

This deviation from the trends observed in VCAM trials was unexpected (Blankenberg et al. 2003; Cybulsky et al. 2001; Venegas-Pino et al. 2016). As plaques become more advanced, inflammation increases to promote macrophage recruitment to the subendothelial space and facilitate lipid clearance (Ruifrok & Johnston, 2001). This recruitment is in part facilitated by VCAM and ICAM, which are responsible for firm adhesion to leukocytes before endothelial extravasation (Cybulsky et al. 2001; Ruifrok & Johnston, 2001; Venegas-Pino et al. 2016). One might reasonably expect both VCAM and ICAM to increase as the plaque progresses, however VCAM demonstrated no significant rise in ApoE$^{-/-}$ Ins2$^{+/Akita}$ mice between 5, 10, 15 and 25 weeks or ApoE$^{-/-}$ mice between 15 and 25 weeks (Noyman et al. 2002). Overall, ApoE$^{-/-}$ mice showed a significant rise in VCAM expression similar to what is seen in ApoE$^{-/-}$ and ApoE$^{-/-}$ Ins2$^{+/Akita}$ in the ICAM trials. VCAM trials of ApoE$^{-/-}$ Ins2$^{+/Akita}$ mice are the only group to show no significant changes between 5 and 25 weeks of age, instead remaining relatively elevated for all time points (Cybulsky et al. 2001). Cybulsky et al. found VCAM, but not ICAM, played an important role in early atherosclerosis (Cybulsky et al. 2001). These findings seem to support their conclusions that VCAM is an independent and key actor in the initiation of atherosclerosis by hyperglycemia.

One should also consider the differences in IHC and IF staining as a possible reason for these differences. 5, 10, 15, and 25-week mice were stained together under the same conditions for ICAM IHC (Ruifrok & Johnston, 2001). The use of IHC methods in lieu of IF could explain these unusual differences; however, the specific staining demonstrated by

the DAB chromogen strictly localized along the endothelium seems evident of its efficacy (Cybulsky et al. 2001; Ruifrok & Johnston, 2001).

Macrophage Recruitment

Similarly, to VCAM, immunofluorescent microscopy of macrophage recruitment with anti-Mac3 showed a marked increase in fluorescent macrophages recruited to atheroprone regions of the subendothelial space in ApoE$^{-/-}$ Ins2$^{+/Akita}$ mice at 5 weeks relative to ApoE$^{-/-}$ mice (Figure 18). By 10 weeks, ApoE$^{-/-}$ mice showed similar macrophage recruitment to ApoE$^{-/-}$ Ins2$^{+/Akita}$ mice at 5 weeks. As we saw in our VCAM trials, ApoE$^{-/-}$ Ins2$^{+/Akita}$ mice demonstrated significantly higher VCAM at 5 and 10 weeks than ApoE$^{-/-}$ mice, before ApoE$^{-/-}$ mice reached similar levels by 15 and 25 weeks of age. Since VCAM is a cellular adhesion molecule tasked with recruiting macrophages to sites of inflammation in the vasculature, it is understandable why macrophage recruitment is similarly higher at 5 weeks in ApoE$^{-/-}$ Ins2$^{+/Akita}$ mice than ApoE$^{-/-}$ mice, however the rise of ApoE$^{-/-}$ macrophage recruitment to similar levels as ApoE$^{-/-}$ Ins2$^{+/Akita}$ mice at 10 weeks is unexpected, as VCAM coverage is still significantly higher in the ApoE$^{-/-}$ Ins2$^{+/Akita}$ mice (Cybulsky et al. 2001). One would expect the macrophage recruitment to remain significantly higher in the ApoE$^{-/-}$ Ins2$^{+/Akita}$ mice where VCAM is also elevated, however this is not the case. This earlier recruitment of macrophages to the subendothelial space helps to illustrate the unique role played by VCAM in the development of early atherosclerosis (Cybulsky et al. 2001).

Conclusions

Hyperglycemia increases the early expression of VCAM but not ICAM, macrophage recruitment in the subendothelial space, and larger atherosclerotic plaques in

ApoE$^{-/-}$ mice. These findings are consistent with evidence that VCAM functions as an important endothelial recruitment factor that plays a unique role in the acceleration of atherosclerosis by hyperglycemia. These results further our insight into the mechanisms behind hyperglycemia, its effect on plaque formation, and highlight the importance of VCAM in early macrophage recruitment and atherosclerotic progression.

Chapter 5: General Discussion

Discussion:

Despite heightened awareness and research into heart disease and stroke, cardiovascular disease remains the primary cause of death worldwide (Das & Elbein, 2006). Type 1 and type 2 diabetes are each independent and strong risk factors for cardiovascular disease, and the growing prevalence of type 1 and type 2 diabetes in the world today should highlight the importance of research into understanding the pathogenesis of atherosclerosis, potential therapeutic targets for medical interventions and clinical applications, prophylactic changes to modifiable risk factors like dietary and lifestyle changes, and such daily and often underestimated essentials, like nutrition and metabolism (Das & Elbein, 2006; Ross, 1993; Yang et al. 2013).

To pursue research in this endeavour, it is essential to find the right animal model. It is often difficult to mirror human conditions in mice, given the differences in size, metabolism, and lifestyle, and so it is important to understand the parameters with which we design our experiments. This study reinforces that dyslipidemia is necessary to induce atherosclerosis in mice and that, while hyperglycemia can accelerate atherosclerosis, it is not sufficient to induce its initiation in normolipidemic $ApoE^{+/-}$ mice (Barber et al. 2005).

When hyperglycemia and dyslipidemia are both present, in $ApoE^{-/-}$ $Ins2^{+/Akita}$ mice, mice develop accelerated atherosclerosis and show elevated expression of VCAM from as early as 5 weeks, and all other ages tested. Where hyperglycemia is absent, we see a gradual rise in VCAM expression over time in dyslipidemic $ApoE^{-/-}$ mice, similar to what was seen with ICAM in both hyperglycemic and normoglycemic mice with dyslipidemia. These results seem to reaffirm the findings of Cybulsky et al. that VCAM, but not ICAM, plays

an important role in early atherosclerosis. Elevated VCAM expression at 5 weeks of age was consistent with earlier influx of macrophages into the subendothelial space at 5 weeks. While macrophage presence in the subendothelial space became similar between normoglycemic and hyperglycemic mice at 10 weeks, this still seems to suggest that chronic hyperglycemia, as seen in diabetes, leads to earlier initiation of plaque formation.

It is especially interesting that VCAM plays such a unique role in this recruitment. It may suggest that suppression of VCAM expression could be a viable avenue of suppressing atherogenesis. Cybulsky et al. found promising results reducing plaque volume when compromising VCAM, however we must also acknowledge the essential role VCAM plays in the recruitment of macrophages to site of inflammation along the endothelium and in other cells. Reduction in the functionality of VCAM could lead to complications with the general immune response, leukocyte-endothelial cell signalling, and disrupt even some mesenchymal stem cells (Shimomura et al. 1999). Leaving ICAM intact may help to mitigate the damage of such therapies, however more research into the matter is needed. For now, this study serves as invaluable information for further analysis of the role of VCAM in the initiation and progression of atherosclerosis in mice.

Conclusions:

This study shows that hyperglycemia increases early VCAM, but not ICAM, expression in ApoE$^{-/-}$ mice; macrophage recruitment to the subendothelial space is also enhanced in hyperglycemic mice; and hyperglycemic mice develop larger plaques that become evident at 25 weeks of age. These findings are consistent with evidence that VCAM functions as an important endothelial recruitment factor that plays a unique role in the acceleration of atherosclerosis by hyperglycemia. These results further our insight into

the mechanisms behind hyperglycemia, its effect on plaque formation, and highlight the importance of VCAM in early macrophage recruitment and atherosclerotic progression independent of ICAM.

Chapter 6: Future Work

Future Directions:

This study discovered a much about the nature of VCAM and dyslipidemia in the progression of early atherosclerosis, however it provides many avenues for further research in its conclusions. Further testing of the gluconormalizing and non-gluconormalizing effects of the $ApoE^{-/-}$ and $ApoE^{+/-}$ hyperglycemic mice respectively could better help us to understand and study female models of hyperglycemia and atherosclerosis in the murine heart and vasculature (Barber et al. 2005). Studies might also wish to look into the effects on mice younger than 5 weeks to see if VCAM is expressed at the same high levels we see at 5, 10, 15, and 25 weeks from birth or when it begins to be evident. Taking samples at 1, 2, 3, and 4 weeks of age could determine how early this effect is observed and whether this phenomenon is present from birth or has a later point of onset. Similar studies into the recruitment of macrophages at these time points would be an excellent way to gauge if their recruitment is chronic from birth or begins atherogenesis at the 5-week time point shown here in hyperglycemic $ApoE^{-/-}$ mice.

Similarly, it may be useful to study the expression of VCAM and ICAM at earlier time points in the $ApoE^{+/-}$ mouse model. Mice in the $ApoE^{-/-}$ model demonstrated greater VCAM expression at 5 and 10 weeks of age, however $ApoE^{+/-}$ mice were only sampled at 25 weeks of age. Further studies should examine the aortic sinus or ascending aorta at 5 and 10 weeks of age in the $ApoE^{+/-}$. This study suggests that dyslipidemia is necessary for hyperglycemia-accelerated plaque growth in mice, however it is unclear if VCAM is still overexpressed at these early ages in a normolipidemic model. It would be interesting to see if one can see elevated levels of VCAM without dyslipidemia.

Studies could also attempt to reaffirm ICAM results with immunofluorescent microscopy in addition to the immunohistochemical DAB staining shown here. While our available antibodies were best suited for the latter method, comparisons with immunofluorescence may further test the activity of ICAM in hyperglycemic mice at both early and advanced stages of atherosclerosis.

It may also be useful to examine the unexpected trends in VCAM fluorescence over time. While we expected VCAM to increase with greater inflammation and plaque progression, it seemed to reach a sort of threshold between 40% and 80% coverage that was maintained in the hyperglycemic mice from 5 weeks to 25 weeks of age, and reached by the normoglycemic mice by 15 and 25. Studies may wish to further analyze the apparent maximal threshold of VCAM expression in the aortic sinus and see if this is both confirmed and present in other areas of the vasculature, like further along the ascending aorta or in later stages of atherosclerotic progression. Similar studies might test the expression of VCAM in cultured endothelial cells. Further analysis of this may test the all-or-none model of VCAM expression in endothelial cells discussed earlier as a possible theory behind the similarity in intensity of VCAM expression per unit area despite greater coverage.

Further research into hyperglycemia, diabetes and cardiovascular disease is essential to address the main source of mortality in the world today. Answering the questions here and expanding our knowledge of pathology and treatment remains one of the most pressing issues in medical science today. The number of people diagnosed with diabetes has risen from 108 million in 1980 to 422 million in 2014 and that number is only rising[1]. More research could better inform the public about prophylactic measures, lifestyle

choices, and management techniques that can continue to better quality of life and longevity for everyone, especially patients with diabetes.

References:

Aronson, D., & Rayfield, E. J. (2002). How hyperglycemia promotes atherosclerosis: molecular mechanisms. *Cardiovascular diabetology*, *1*(1), 1.

Baker, R. G., Hayden, M. S., & Ghosh, S. (2011). NF-κB, inflammation, and metabolic disease. *Cell metabolism*, *13*(1), 11-22.

Barber, A. J., Antonetti, D. A., Kern, T. S., Reiter, C. E., Soans, R. S., Krady, J. K., Levison S. W., Gardner T. W. & Bronson, S. K. (2005). The Ins2Akita mouse as a model of early retinal complications in diabetes. *Investigative ophthalmology & visual science*, *46*(6), 2210-2218.

Barreiro, O., Yáñez-Mó, M., Serrador, J. M., Montoya, M. C., Vicente-Manzanares, M., Tejedor, R., ... & Sánchez-Madrid, F. (2002). Dynamic interaction of VCAM-1 and ICAM-1 with moesin and ezrin in a novel endothelial docking structure for adherent leukocytes. *The Journal of cell biology*, *157*(7), 1233-1245.

Basta, G., Schmidt, A. M., & De Caterina, R. (2004). Advanced glycation end products and vascular inflammation: implications for accelerated atherosclerosis in diabetes. *Cardiovascular research*, *63*(4), 582-592.

Beckman, J. A., Creager, M. A., & Libby, P. (2002). Diabetes and atherosclerosis: epidemiology, pathophysiology, and management. *Jama*, *287*(19), 2570-2581.

Beriault, D. R., Dang, V. T., Zhong, L. H., Petlura, C. I., McAlpine, C. S., Shi, Y., & Werstuck, G. H. (2016). Glucosamine induces ER stress by disrupting lipid-linked oligosaccharide biosynthesis and N-linked protein glycosylation. *American Journal of Physiology-Endocrinology and Metabolism*, ajpendo-00275.

Black, T. M., Wang, P., Maeda, N., & Coleman, R. A. (2000). Palm tocotrienols protect ApoE+/− mice from diet-induced atheroma formation. *The Journal of nutrition*, *130*(10), 2420-2426.

Blankenberg, S., Barbaux, S., & Tiret, L. (2003). Adhesion molecules and atherosclerosis. *Atherosclerosis*, *170*(2), 191-203.

Braun, A., Zhang, S., Miettinen, H. E., Ebrahim, S., Holm, T. M., Vasile, E., ... & Andrews, N. C. (2003). Probucol prevents early coronary heart disease and death in the high-density lipoprotein receptor SR-BI/apolipoprotein E double knockout mouse. *Proceedings of the National Academy of Sciences*, *100*(12), 7283-7288.

Brownlee, M., Cerami, A., & Vlassara, H. (1988). Advanced glycosylation end products in tissue and the biochemical basis of diabetic complications. *New England Journal of Medicine*, *318*(20), 1315-1321.

Ceriello, A., Falleti, E., Motz, E., Taboga, C., Tonutti, L., Ezsol, Z., ... & Bartoli, E. (1998). Hyperglycemia-induced circulating ICAM-1 increase in diabetes mellitus: the possible role of oxidative stress. *Hormone and Metabolic Research*, *30*(03), 146-149.

Chen, M. S., Hutchinson, M. L., Pecoraro, R. E., Lee, W. Y., & Labbé, R. F. (1983).

Hyperglycemia-induced intracellular depletion of ascorbic acid in human mononuclear leukocytes. *Diabetes*, *32*(11), 1078-1081.

Coleman, D. L., Schwizer, R. W., & Leiter, E. H. (1984). Effect of genetic background on the therapeutic effects of dehydroepiandrosterone (DHEA) in diabetes-obesity mutants and in aged normal mice. *Diabetes*, *33*(1), 26-32.

Cybulsky, M. I., Iiyama, K., Li, H., Zhu, S., Chen, M., Iiyama, M., ... & Milstone, D. S. (2001). A major role for VCAM-1, but not ICAM-1, in early atherosclerosis. *The Journal of clinical investigation*, *107*(10), 1255-1262.

D'Agostino, R. B., Belanger, A., & D'Agostino Jr, R. B. (1990). A suggestion for using powerful and informative tests of normality. *The American Statistician*, *44*(4), 316-321.

Das, S. K., & Elbein, S. C. (2006). The genetic basis of type 2 diabetes. *Cellscience*, 2(4), 100.

Falk, E. (2006). Pathogenesis of atherosclerosis. *Journal of the American College of Cardiology*, *47*(8 Supplement), C7-C12.

Feener, E. P., & King, G. L. (1997). Vascular dysfunction in diabetes mellitus. *The Lancet*, *350*, S9-S13.

Funk, S. D., Yurdagul, A., & Orr, A. W. (2012). Hyperglycemia and endothelial dysfunction in atherosclerosis: lessons from type 1 diabetes. *International journal of vascular medicine*, *2012*.

Gabbay, K. H., Hasty, K., Breslow, J. L., Ellison, R. C., Bunn, H. F., & Gallop, P. M. (1977). Glycosylated hemoglobins and long-term blood glucose control in diabetes mellitus. *The Journal of Clinical Endocrinology & Metabolism*, *44*(5), 859-864.

Gerlis, L. M., Davies, M. J., Boyle, R., Williams, G., & Scott, H. (1985). Pre-excitation due to accessory sinoventricular connexions associated with coronary sinus aneurysms. A report of two cases. *Heart*, *53*(3), 314-322.

Graham, M. L., Janecek, J. L., Kittredge, J. A., Hering, B. J., & Schuurman, H. J. (2011). The streptozotocin-induced diabetic nude mouse model: differences between animals from different sources. *Comparative medicine*, *61*(4), 356-360.

Haynes, W. (2013). Student's t-test. In *Encyclopedia of Systems Biology* (pp. 2023-2025). Springer, New York, NY.

Heiberger, R. M., & Neuwirth, E. (2009). One-way anova. In *R through excel* (pp. 165-191). Springer, New York, NY.

Heron, M. P. (2018). Deaths: leading causes for 2016.Kannel, W. B., & McGee, D. L. (1979). Diabetes and cardiovascular disease: the Framingham study. *Jama*, *241*(19), 2035-2038.

Karpen, C. W., Cataland, S., O'dorisio, T. M., & Panganamala, R. V. (1985). Production of 12-hydroxyeicosatetraenoic acid and vitamin E status in platelets from type I human diabetic subjects. *Diabetes*, *34*(6), 526-531.

Khalfaoui, T., Lizard, G., & Ouertani-Meddeb, A. (2008). Adhesion molecules (ICAM-1 and VCAM-1) and diabetic retinopathy in type 2 diabetes. *Journal of molecular histology*, *39*(2), 243-249.

Maeda, N. (2011). Development of apolipoprotein E–deficient mice. *Arteriosclerosis, thrombosis, and vascular biology*, *31*(9), 1957-1962.

Marlin, S. D., & Springer, T. A. (1987). Purified intercellular adhesion molecule-1

(ICAM-1) is a ligand for lymphocyte function-associated antigen 1 (LFA-1). *Cell*, *51*(5), 813-819.

Maron, B. A., & Michel, T. (2012). Subcellular localization of oxidants and redox modulation of endothelial nitric oxide synthase. *Circulation Journal*, *76*(11), 2497-2512.

Martin-Body, R. L., Robson, G. J., & Sinclair, J. D. (1985). Respiratory effects of sectioning the carotid sinus glossopharyngeal and abdominal vagal nerves in the awake rat. *The Journal of Physiology*, *361*(1), 35-45.

Matthys, K. E., & Bult, H. (1997). Nitric oxide function in atherosclerosis. *Mediators of inflammation*, *6*(1), 3-21.

McKnight, P. E., & Najab, J. (2010). Kruskal-Wallis Test. *The corsini encyclopedia of psychology*, 1-1.

McKnight, P. E., & Najab, J. (2010). Mann-Whitney U Test. *The Corsini encyclopedia of psychology*, 1-1.

Moore, K. J., Sheedy, F. J., & Fisher, E. A. (2013). Macrophages in atherosclerosis: a dynamic balance. *Nature Reviews Immunology*, *13*(10), 709.

Newham, P., Craig, S. E., Seddon, G. N., Schofield, N. R., Rees, A., Edwards, R. M., ... & Humphries, M. J. (1997). α4 integrin binding interfaces on VCAM-1 and MAdCAM-1 integrin binding footprints identify accessory binding sites that play a role in integrin specificity. *Journal of Biological Chemistry*, *272*(31), 19429-19440.

Nguyen, D., Dhanasekaran, P., Phillips, M. C., & Lund-Katz, S. (2009). Molecular mechanism of apolipoprotein E binding to lipoprotein particles. *Biochemistry*, *48*(13), 3025-3032.

Nishikawa, T., Edelstein, D., Du, X. L., Yamagishi, S. I., Matsumura, T., Kaneda, Y., ... & Giardino, I. (2000). Normalizing mitochondrial superoxide production blocks three pathways of hyperglycaemic damage. *Nature*, *404*(6779), 787.

Noyman, I., Marikovsky, M., Sasson, S., Stark, A. H., Bernath, K., Seger, R., & Madar, Z. (2002). Hyperglycemia reduces nitric oxide synthase and glycogen synthase activity in endothelial cells. *Nitric Oxide*, *7*(3), 187-193.

Poirier, B., Bidouard, J. P., Cadrouvele, C., Marniquet, X., Staels, B., O'connor, S. E., ... & Herbert, J. M. (2005). The anti-obesity effect of rimonabant is associated with an improved serum lipid profile. *Diabetes, Obesity and Metabolism*, *7*(1), 65-72.

Rashid, S., Curtis, D. E., Garuti, R., Anderson, N. N., Bashmakov, Y., Ho, Y. K., ... & Horton, J. D. (2005). Decreased plasma cholesterol and hypersensitivity to statins in mice lacking Pcsk9. *Proceedings of the National Academy of Sciences*, *102*(15), 5374-5379.

Ross, R. (1993). The pathogenesis of atherosclerosis: a perspective for the 1990s.

Rousseeuw, P. J., & Leroy, A. M. (2005). *Robust regression and outlier detection* (Vol. 589). John Wiley & Sons.

Ruifrok, A. C., & Johnston, D. A. (2001). Quantification of histochemical staining by color deconvolution. *Analytical and quantitative cytology and histology*, *23*(4), 291-299.

Shea, T. B., Ortiz, D., & Rogers, E. (2004). Differential susceptibity of transgenic mice lacking one or both apolipoprotein alleles to folate and vitamin E deprivation. *Journal of Alzheimer's Disease*, *6*(3), 269-273.

Shimomura, I., Bashmakov, Y., & Horton, J. D. (1999). Increased levels of nuclear

SREBP-1c associated with fatty livers in two mouse models of diabetes mellitus. *Journal of Biological Chemistry*, *274*(42), 30028-30032.

Sud, A., Parker, F., & Magilligan, D. J. (1984). Anatomy of the aortic root. *The Annals of thoracic surgery*, *38*(1), 76-79.

The Jackson Laboratory Mouse Strain Datasheet. (2018). *C57BL/6-Ins2Akita/J Mouse Datasheet*. [online] Available at: https://www.jax.org/strain/003548 [Accessed 9 Jul. 2018].

Thum, T., Fraccarollo, D., Schultheiss, M., Froese, S., Galuppo, P., Widder, J. D., ... & Bauersachs, J. (2007). Endothelial nitric oxide synthase uncoupling impairs endothelial progenitor cell mobilization and function in diabetes. *Diabetes*, *56*(3), 666-674.

Vacek, T. P., Rehman, S., Neamtu, D., Yu, S., Givimani, S., & Tyagi, S. C. (2015). Matrix metalloproteinases in atherosclerosis: role of nitric oxide, hydrogen sulfide, homocysteine, and polymorphisms. *Vascular health and risk management*, 11, 173.

Vásquez-Vivar, J., Kalyanaraman, B., MARTAsek, P. A. V. E. L., Hogg, N., Masters, B. S. S., Karoui, H., ... & Pritchard, K. A. (1998). Superoxide generation by endothelial nitric oxide synthase: the influence of cofactors. *Proceedings of the National Academy of Sciences*, *95*(16), 9220-9225.

Venegas-Pino, D. E., Banko, N., Khan, M. I., Shi, Y., & Werstuck, G. H. (2013). Quantitative analysis and characterization of atherosclerotic lesions in the murine aortic sinus. *Journal of visualized experiments: JoVE*, (82).

Venegas-Pino, D. E., Wang, P. W., Stoute, H. K., Singh-Pickersgill, N. A., Hong, B. Y., Khan, M. I., ... & Werstuck, G. H. (2016). Sex-Specific Differences in an ApoE−/−: Ins2+/Akita Mouse Model of Accelerated Atherosclerosis. *The American journal of pathology*, *186*(1), 67-77.

Walpola, P. L., Gotlieb, A. I., Cybulsky, M. I., & Langille, B. L. (1995). Expression of ICAM-1 and VCAM-1 and monocyte adherence in arteries exposed to altered shear stress. *Arteriosclerosis, thrombosis, and vascular biology*, *15*(1), 2-10.

Watanabe, T., Tokunaga, O., Fan, J., & Shimokama, T. (1989). Atherosclerosis and macrophages. *Pathology International*, *39*(8), 473-486.

Wu, K. K., & Huan, Y. (2007). Diabetic atherosclerosis mouse models. *Atherosclerosis*, *191*(2), 241-249.

Yang, Z. X., Han, Z. B., Ji, Y. R., Wang, Y. W., Liang, L., Chi, Y., ... & Chen, D. D. (2013). CD106 identifies a subpopulation of mesenchymal stem cells with unique immunomodulatory properties. *PloS one*, *8*(3), e59354.

Zadelaar, S., Kleemann, R., Verschuren, L., de Vries-Van der Weij, J., van der Hoorn, J., Princen, H. M., & Kooistra, T. (2007). Mouse models for atherosclerosis and pharmaceutical modifiers. *Arteriosclerosis, thrombosis, and vascular biology*, *27*(8), 1706-1721.

Zhang, S. H., Reddick, R. L., Burkey, B., & Maeda, N. (1994). Diet-induced atherosclerosis in mice heterozygous and homozygous for apolipoprotein E gene disruption. *The Journal of clinical investigation*, *94*(3), 937-945.

Zhang, S. H., Reddick, R. L., Piedrahita, J. A., & Maeda, N. (1992). Spontaneous hypercholesterolemia and arterial lesions in mice lacking apolipoprotein E. *Science*, *258*(5081), 468-471.